ISSN 0736-5306

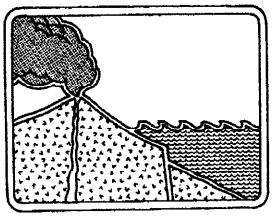

SCIENCE OF TSUNAMI HAZARDS

The International Journal of The Tsunami Society

Volume 17 Number 1 1999

FIRST TSUNAMI SYMPOSIUM PAPERS

OBJECTIVE: **The Tsunami Society** publishes this journal to increase and disseminate knowledge about tsunamis and their hazards.

DISCLAIMER: Although these articles have been technically reviewed by peers, **The Tsunami Society** is not responsible for the veracity of any statement, opinion or consequences.

Submit manuscripts of articles, notes or letters to the Editor. If an article is accepted for publication the author(s) must submit a camera ready manuscript in the journal format. A voluntary $30.00 page charge for Tsunami Society members, $50.00 for non-members will include 50 reprints.

SUBSCRIPTION INFORMATION: Price per copy $20.00 USA

 Previous issues of the journal are available in PDF format at **http://epubs.lanl.gov/tsunami/** and on a CD-ROM from the Society.

ISSN 0736-5306 **http://www.ccalmr.ogi.edu/STH**

Published by The Tsunami Society in Honolulu, Hawaii, USA

FINITE ELEMENT MODELING OF POTENTIAL CASCADIA SUBDUCTION ZONE TSUNAMIS

Edward P. Myers and António M. Baptista
Center for Coastal and Land-Margin Research
Department of Environmental Science and Engineering
Oregon Graduate Institute of Science & Technology
P.O. Box 91000
Portland, OR 97291-1000

George R. Priest
Oregon Department of Geology and Mineral Industries
Suite 965, 800 NE Oregon St. #28
Portland, OR 97232

ABSTRACT

Evidence of historic Cascadia Subduction Zone earthquakes and subsequent tsunamis have prompted hydrodynamic modeling efforts to identify potential flow patterns and coastal hazards for plausible future events. In this study we identify the methods used to derive potential seismic source scenarios and present a thorough evaluation of finite element simulations of the tsunamis associated with those scenarios. The first part of this paper deals with regional impacts of potential tsunamis, while the second part evaluates the fate of the modeled waves from the local perspectives of Seaside, OR and Newport, OR. Both parts are composed of physical as well as numerical interpretations of the simulations.

Note: A more comprehensive version of this article,
http://www.ccalmr.ogi.edu/STH/online/volume17/number1/mbp/
is available from the Science of Tsunami Hazards web site. The web version contains more extensive results and analyses for each of the tsunami scenarios considered in this study, and includes selected color plots and animations.

INTRODUCTION

The Cascadia Subduction Zone, located off the northwest coast of the United States and Vancouver Island, has generated large earthquakes and tsunamis approximately every 200-600 years. The last of these events occurred about 300 years ago. The geologic evidence supporting these past events is summarized by Atwater et al. (1995).

Using available geophysical and geological data from the Cascadia Subduction Zone, this modeling study aims to reproduce deformations from potential earthquakes and to simulate their ensuing tsunamis as an indicator of future hazards for Oregon and Washington coastal communities. The modeled tsunamis will be analyzed from both regional and local perspectives. Regional analyses should identify the influence of bathymetry and coastline geometry on elevation, velocity, and wave frequency patterns throughout the domain.

While regional perspectives permit identification of energy focusing mechanisms as the tsunami approaches the coastline, local perspectives are equally important in analyzing what happens to the waves as they interact with the coastline. For example, the 1992 Nicaragua tsunami wave runup observations made by Baptista et al. (1993) indicate that some localities and embayments were subjected to very heterogeneous runup observation differences. Local coastline geometry, bathymetry, topography, and resonance conditions can affect the behavior of the waves as they interact between the coast and the continental shelf. To investigate such local phenomena, the finite element grid resolution needs be adequate enough to handle the rapidly changing nature of velocities and elevations in these regions. Such resolution is implemented in the areas of Seaside, OR and Newport, OR, and the modeling results are evaluated in detail for these communities.

While eight earthquake scenarios (named 1A, 1B, 1C, 2A, 2B, 2C, 2CN, and 2CS) were considered in this study, only results from scenario 1A will be presented here. The corresponding web page journal article (http://www.ccalmr.ogi.edu/STH/online/volume17/number1/mbp/), however, provides analyses of results for each of the scenarios.

The physical interpretation of modeling results will provide clues to the determining factors in the fate of tsunami waves. The numerical interpretation, likewise, is a critical component in helping to assess the usefulness of numerical models in evaluating and mitigating tsunami hazards. The identification of the limits of a numerical model and how those limits can be minimized will in turn allow the physical mechanisms to be better represented and the mitigation to be more effective. It is the mitigation, after all, which is the end result of a study such as this. For example, the state of Oregon is utilizing these results in accordance with State Senate Bill 379 to estimate potential inundation patterns resulting from Cascadia tsunamis. To combine deformation estimates, hydrodynamic models for the tsunamis, and physical interpretation of results for the purpose of hazard mitigation, each component is scrutinized in the remaining sections.

INITIAL CONDITIONS: DEFORMATION

Finite element simulations of tsunamis are dependent upon the sea floor deformation resulting from the subduction earthquake. This deformation maps itself through the water column and is therefore treated as an initial condition in the hydrodynamic modeling of the tsunami. Wave and velocity patterns are thus highly dependent upon the assumed deformation along the ocean floor. This deformation must be computed through the use of dislocation models such as those presented by Okada (1985) and Mansinha and Smylie (1971). Dislocation models use fault parameters such as the length, width, dip angle, strike direction, rake angle, and slip to compute the deformation in an elastic half-space. Deformation patterns for most tsunami modeling applications have historically been computed by either assuming some characteristic shape (Hebenstreit and Murty 1989, Ng et al. 1990) or by using a dislocation model that

assumes a rectangular fault locked over its entire area prior to rupture (Myers and Baptista 1995, Whitmore 1993). The magnitudes of tsunami waves generated using the latter approach, as compared with tide gauge responses, demonstrate that the deformations appear to be the right order of magnitude. However, there is significant ambiguity incorporated in the assumptions of the fault parameters as well as the location of the locked zone.

A better approach is to incorporate the wide range of three-dimensional heterogeneity of the fault zone into the dislocation model, and to allow transition zones where the slip will be less than that occurring in the fully locked zone. Flück et al. (1997) permit such an approach by not relying on the typical rectangular source formulas for computing deformation in an elastic half-space. Instead, the subduction is represented by the integration of many point sources throughout the subduction zone. Okada (1985) provides the necessary formulas for computing the deformation from either a point source or a rectangular source. Using the algorithm and program provided by Flück et al. (1997), it is feasible to computationally break the fault up into a grid of triangular elements. The nodes of these elements contain information about the horizontal and vertical positions of the fault at that point. Over each triangle, the slip and direction of convergence are specified, which permits varying amounts of slip to be distributed in different regions of the fault zone.

Geist and Yoshioka (1996) followed a similar approach to modeling the deformation by using a three-dimensional elastic finite element model. In that study, rupture along five different types of faults was considered for the Cascadia Subduction Zone. These included interplate thrust (rupture along the locked zoned), décollement (rupture updip of the locked zone), landward and seaward vergent thrust faults (rupture along abrupt branches from the décollement to the surface), and prominent thrust fault rupture near the edge of the continental shelf. The seaward vergent faulting mechanism is theorized (Fukao, 1979) to be characteristic of tsunami earthquakes (earthquakes which generate unusually large tsunamis as compared to the seismic moment). Geist and Yoshioka then use the resulting deformation from each of these faulting mechanisms to simulate possible tsunami impacts from each scenario, assuming different seismic parameters.

The most probable generating mechanisms for tsunamigenic earthquakes in the Cascadia margin appear to be interplate and décollement thrust type faults. Therefore, these two mechanisms are evaluated in the contexts shown in Figure 1. Three scenarios are evaluated, each of which varies with respect to how the slip is distributed over the seaward transition, locked, and landward transition zones. The first scenario assumes that the locked zone actually extends all the way up to the surface of the sea floor (scenario A). The second assumes that there is a seaward transition zone in which the slip varies linearly (scenario B). The third assumes that there is a seaward transition zone, but that no slip is occurring in this zone (scenario C). Each slip scenario assumes that a landward transition zone exists downdip of the locked zone in which the slip varies decreases linearly.

Two different cases will be considered, with each case consisting of the three slip scenarios mentioned above. The cases differ only in the placement of the 350° and 450° isotherms. The 350° isotherm is believed to represent the downdip extent of the locked zone due to the onset of quartz plasticity, and the 450° isotherm is theorized to represent the downdip limit of the stable sliding transition zone associated with the onset of feldspar plasticity (Hyndman and Wang, 1993). The first case (case 1, combined with the above slip scenarios: 1A, 1B, and 1C) assumes the positions of these two isotherms from Hyndman and Wang's (1995) finite element model of the thermal regime. The second case (case 2, combined with the above slip scenarios: 2A, 2B, 2C) positions these two isotherms based on paleoseismic evidence. While Hyndman and Wang's isotherms are well constrained north of the Columbia River by geophysical data, poorer constraints south of this point lead to greater uncertainties, particularly in terms of comparisons with estimates of the deformation from paleoseismic data. Priest (1995) concluded that south of the Columbia River, it would be more appropriate to use limits for the landward transition zone which are different from the 350° and 450° isotherms of Hyndman and Wang. Priest derived such limits based upon paleoseismic data and previous deformation models in the Cascadia Subduction Zone. Thus, the second case considered will use Priest's limits for the landward transition zone south of the Columbia

River. It should be reiterated that both cases consider three different scenarios that differ in the way slip is distributed in the seaward transition zone, the locked zone, and the landward transition zone. The isotherms for both cases are shown in Figure 2 along with the positions of the surface of the fault zone and the seaward transition zone that were provided by Goldfinger (1996).

In addition to these six deformation models, shorter segment breaks are also considered. In 1995, Geomatrix Consultants performed a probabilistic acceleration map for the state of Oregon, which included probability estimates of the type and recurrence interval of Cascadia Subduction Zone earthquakes. This study concluded that a rupture length of 450 km was most probable. Despite the fact that geologic evidence indicates recurrence intervals longer than 300 years, the probability study concluded that for a 450 km rupture length, a 225 year recurrence interval should be assumed. Using locations of local marine terraces and faults, Priest et al. (1997) concluded that 450 km rupture scenarios should be bounded (either above or below) by the 44.8° latitude near Depoe Bay, Oregon. Segment scenarios based on the case 2 isotherms will be considered both to the north and to the south of this latitude, extending 450 km in length (2CN and 2CS).

The depths of the Cascadia Subduction Zone fault were provided by Flück et al. (1997). The dip angles of the fault zone are calculated using these fault depths in the dislocation model. The magnitude and direction of slip for each node in the deformation grid were computed using convergence rates between the plates (program provided by Kanamori, 1996). Utilizing the North America-Juan de Fuca Euler vector computed by DeMets et al. (1990), slip magnitudes and directions were computed assuming a 450 year interval between earthquakes. The 2CN and 2CS scenarios, however, assumed a 225 year interval.

The deformation pattern for scenario 1A is shown in Figure 3. The width of the deformation region is larger in Washington, particularly northern Washington. Cross sections of deformation at the latitude of Newport, OR are shown in Figure 4a for all of the scenarios considered. A similar graph of cross sections at the latitude of Seaside, OR is presented in Figure 4b. Scenarios 1A and 2A (fully locked to the surface) have large peaks of uplift near the deformation front. Case 2 has more volume of uplift for the three slip scenarios than Case 1, and the region of subsidence for Case 2 is located further towards the land than Case 1.

DESCRIPTION OF THE MODEL: GOVERNING EQUATIONS

In this study, the finite element model ADCIRC (Luettich et al., 1991) is used to propagate waves in the open ocean until they reach the coastline, at which point inundation is allowed to occur (Luettich and Westerink, 1995a-b). The use of a finite element method for the hydrodynamic modeling allows the discretization to vary depending upon the bathymetric domain and numerical criteria. The coastline and topographic features may also be better approximated, and the seismic source is more accurately depicted in an unstructured grid. The seismic source was imposed in ADCIRC by adjusting the kinematic boundary condition to allow the ocean floor to dynamically move over three time steps. This is essentially equivalent to mapping the bottom deformation into the water column directly.

ADCIRC uses a generalized wave continuity formulation to supplant the primitive continuity equation, a technique that has proven to avoid the spurious $2\Delta x$ oscillations of early finite element applications. The modified generalized wave continuity equation (GWCE) is derived as a summation of the time derivative of the continuity equation, the primitive continuity equation weighted by a factor, and the spatial gradient of the momentum equations expressed in conservative form. The GWCE and momentum equations used by ADCIRC are discussed in Luettich et al. (1991), Myers and Baptista (1995), and the web version of this paper.

MODELING RESULTS

Grid Setup

The semi-automatic grid generator, ACE/gredit (Turner and Baptista, 1991), permits interactive development of finite element grids. Such a flexible tool is critical in assembling a grid, as the manner in which elements are interconnected will influence the amount of numerical error introduced during a simulation. The size of the elements throughout the grid should be proportional to the depths, and transitioning from large elements to small elements helps to ensure numerical soundness. In addition, elements on land that may be inundated need to be much smaller (than wet elements) in order to facilitate a better representation of the wetting and drying process.

Using these criteria, two different grids for tsunami simulations were used in this study. Grid 1 is displayed in Figure 5a and extends from the Aleutian Islands to central California. Grid 2 is displayed in Figure 5b and extends between northern Washington and northern California. Both Grid 1 and Grid 2 have the same level of refinement in the Seaside and Newport regions. These two communities were selected to evaluate the local behavior of the waves in the estuaries and as the waves inundate the land. Figure 6 portrays the differences between the two grids near Seaside. The grids are virtually the same, except Grid 2 has more refinement in deeper waters and along the coastline outside of the Seaside region. If the Grid 1 resolution is insufficient to propagate all the frequencies of the tsunami, then such insufficiencies should surface as differences between the results on the two grids. Figures 7a and 7b show enlargements of Seaside and Newport, respectively. The smallest elements are on the order 5-10 meters.

Regional Modeling Results

Results will first be evaluated from a regional perspective, thus permitting a preliminary vantage of what mechanisms affect the propagation of the waves before they reach the shoreline. It should first be mentioned that the Cascadia simulations do not include the influence of tides. The results shown here, rather, were generated assuming that mean higher high water (MHHW) exists throughout the duration of the simulation. MHHW is assumed for safety purposes, because it is instructive to evaluate the impact of the tsunami at maximum water levels. Myers and Baptista (1998a) evaluate nonlinear interactions between tides and tsunamis, the results of which indicate that safety factors should be incorporated to account for such interactions when tides are not directly forced in the simulation.

Bathymetry is the primary feature that will affect the manner in which the tsunami waves are propagated to the coastline. Figure 8 displays some of the bathymetric features for the domain of interest. First, a comparison should be made between this figure and Figure 3. The latter figure shows that the subduction zone extends further away from the coast in the higher latitudes. The exception to this is off the coast of Vancouver Island, but in general the deformation occurs in deeper waters the further north one is located. The implication of this is that waves initially generated in larger depths have more of an opportunity to amplify as they propagate towards the coast. Thus, the initial waves generated off the coast of northern Oregon and Washington will most likely be larger than those generated off the coast of southern Oregon.

Since the rake angle of the fault zone leads to deformations that are oriented almost north to south, the initial waves will be travelling in an approximate west-east manner. The heterogeneities in north-south transects of the bathymetry, therefore, will play an important role in the convergence or divergence of wave energy into certain regions. For example, Figure 8 shows some of the canyons, banks, and valleys throughout the domain that will affect the wave propagation. The shallow banks off the central coast of Oregon, for example, will slow down and amplify the waves passing over them. To the north and south of

these banks, the waves will be traveling faster, thus creating a focusing effect of the entire wave front as it is bent towards the Alsea and Yaquina bay vicinities. Such prominent effects are also present in northern Oregon and Washington, primarily due to canyons protruding into shallower waters.

Figure 9 shows these maximum coastal wave elevations for the seven simulations that were made on Grid 1. Two of the scenarios (1A and 1C) were also simulated using Grid 2, the results of which are included in Figure 9. Recall that Grid 1 and Grid 2 essentially have the same refinement in Newport and Seaside, but Grid 2 has more refinement along the rest of the coastline and through most of the domain.

On grid 1, scenario 1A generally has larger wave heights than 2A, and similarly 1C has larger wave heights than 2C. Most of the differences between "1" and "2" scenarios occur south of Willapa Bay down to California. This area south of Willapa Bay is where the landward transition zone was moved eastward in order to create the "2" cases. Due to this shift of the landward transition zone, the volume of deformation and the amount of subsidence along the ocean floor is larger in the "1" scenarios. The increased volume leads to more displacement of water in the initial waves that in turn could lead to higher runups at the coastline. The more subsidence occurring along the ocean floor for the "1" scenarios could also lead to higher runups, as Tadepalli and Synolakis (1994) have shown that leading depression waves generally lead to larger wave runups onto land.

1A and 1C give fairly similar results for Oregon and California. This is an interesting result, considering the cross sections of deformation shown in Figures 4a and 4b for Newport and Seaside. The shape and position of the 1A and 1C deformation uplifts are different enough to expect different wave heights along the coastline. However, the subsidence for each case is almost identical, and perhaps more importantly, the volume of uplift is almost identical. Above Oregon, 1C shows higher coastal wave elevations than 1A, due to the fact that there is generally more volumetric uplift occurring along the ocean floor in these areas. Results among the 2A, 2B, and 2C scenarios are fairly similar from California through central Oregon. Above central Oregon, the 2A, 2B, and 2C scenarios begin to differ in the volume of uplift occurring: 2C has more volumetric displacement than 2B which has more displacement than 2A. The resulting wave heights are commensurate with this.

Scenarios 2CS and 2CN yield values that are about one half the values of the other scenarios, owing to about half as much deformation. This is due to the fact that 2CN and 2CS assumed only a 225 year interval between earthquakes, as compared to the 450 year interval for the other scenarios. The 2CN simulation resulted in larger wave heights in the northern part of the domain and smaller wave heights in the southern part. The southern wave heights from 2CN resulted from the trapping and propagation of waves along the shelf and coastline. As would be expected, the 2CS simulation yielded higher wave heights in the south than 2CN, but also led to significant waves in northern parts of the domain. Thus it appears that with segmented deformation scenarios, waves have more of a propensity to move north along the coast than they do to move south.

From a numerical modeling perspective, the most interesting results in Figure 9 derive from the differences between simulations made on Grid 1 versus those made on Grid 2. For both 1A and 1C, the Grid 2 simulations led to higher coastal wave elevations. The 1A differences were largest in the southern part of the domain and along the central and northern Oregon coastline. Differences in the 1C simulations were more evenly distributed throughout the entire domain, although larger wave height increases did occur in California and Washington. Clearly, though, energy is being lost in the Grid 1 simulations. This may be due to phenomena such as numerical diffusion, truncation errors, or assumptions in the shallow water equations. The energy may be lost in Grid 1 as the waves reach the coastline and/or as the waves propagate towards the coastline. Myers and Baptista (1998b) dissect the potential sources of such energy loss in tsunami simulations by evaluating nodal energy errors and truncation errors. The importance of these differences is far-reaching for regional tsunami modeling. Both Grid 1 and Grid 2 are approaching 100,000 nodes in the finite element grid. Such grids could not be used a few years ago and are currently pushing the limits of today's state-of-the-art computers.

Analysis of maximum coastal velocity magnitudes (see web version of paper) for the same simulations is commensurate with that of the elevations. One difference of importance, though, is that

velocity magnitudes in Newport and Seaside are larger than for other regions. The reason that the velocities are higher in these two vicinities is most likely associated with the added grid refinement there. The added grid refinement therefore allows the kinetic energy to be better preserved.

Figure 10 displays the isolines of maximum elevation for scenario 1A (see web version of paper for other scenarios). The isolines clearly show where the initial waves were generated, as indicated by the darker regions near the deformation front. More interesting, though, are the visible bathymetric conduits through which the tsunami energy is channeled. Regions of larger elevations, connecting the deformation front to the coastline, can be seen along the shallow banks off of central Oregon and to the north and south of the most prominent canyons (Astoria and Grays canyons). Most of the scenarios show increased wave activity around Crescent City and Humboldt Bay, CA.

Enhanced velocity magnitudes along the shallow banks are also noticeable, as discussed in the web version of the paper. The full segment scenarios demonstrate that higher velocities are witnessed off the coasts of Washington and Vancouver Island. The geometry of the coastline in northern California is such that velocities and elevations appear to be enhanced as the tsunami waves meander along the shoreline and continental shelf.

As mentioned, the results presented in this study assumed an added water level commensurate with mean higher high water. Figure 11 shows the maximum coastal wave elevations for a simulation that was performed with simultaneous imposition of tides and the tsunami. The graph on the right in this figure exemplifies the significance of tide and tsunami interactions. The imposition of the tsunami was arbitrarily chosen to start at some point in the tidal cycle. For this particular tsunami generation time within the tidal cycle, the maximum tsunami elevations in the south seem to generally be damped due to interaction with the trough of the tidal components. However, the timing for this scenario is such that maximum elevations in northern Oregon occur as a result of positive interference between the tide and tsunami waves, thus resulting in larger than expected wave heights. This figure alludes to the importance of tide and tsunami interactions, and future inundation maps should attempt to capture this effect as best possible.

Local Modeling Results

While viewing the results in a regional format aids in interpreting the regional mechanisms that affect the large-scale propagation of the waves, it is also critical to evaluate the fate of the waves as they interact at a more local scale. One of the preliminary ways of viewing results locally is to examine the time history of elevations and velocities at specific points along the coastline. Figures 12a-b display the elevation time histories for points located in approximately five to ten meters depth of water near Newport (Yaquina Bay) and Seaside. Notice the nature of the first waves from each scenario. All of the "1" scenarios commence with an initial trough. Thus, an observer along the shoreline would see the water initially receding and potentially drying some of the seabed. This initial trough is associated with the ocean floor subsidence that is located east of the region of uplift. The "2" scenarios also lead to such a receding of water in the trough of the wave, but only for stations located approximately north of Florence, OR. The majority of subsidence south of this point occurs on land, and uplift is primarily occurring along the ocean floor. Thus, south of Florence, the "2" scenarios show an initial rise in water associated with the incoming positive-elevation wave. This is important, considering the research of Tadepalli and Synolakis (1994) on increased runups associated with leading depression waves.

The web version of this paper shows time histories of elevations and velocities for more locations along the northwest coast of the United States. They show that the maximum wave elevations in each time series generally increase with latitude. This is primarily associated with the fact that the deformation generally occurs further away from the coast in the northern regions. As mentioned earlier, initial waves generated in deeper waters have more of an opportunity to amplify as they move into the shallower waters. Higher wave elevations along central and northern Oregon are also associated with whether the offshore bathymetric contours tend to focus the wave energy towards that region or not. The 1A and 1C

simulations yield similar wave histories, although there is more of a phase difference between the two that varies proportionally with latitude. Similarly the 2A, 2B, and 2C simulations provide similar results at most locations, and there is a phase difference between these wave histories that also varies proportionally with latitude. The 2C waves, in general, have larger amplitudes than 2A, and the 2B elevation time histories are usually situated between the 1A and 2A results.

The time histories of velocity magnitudes display similar trends as observed in the elevation time histories. However, the velocities are particularly stronger in areas that have entrances leading back to bays or estuaries. Examples include Yaquina Bay, the Columbia River, Willapa Bay, and Grays Harbor. As more grid refinement is added to these entrances, the computed velocities are generally higher. The Columbia River appears to be a region in which much of the potential energy is converted to kinetic energy, thus dissipating the wave elevations while amplifying the velocities.

The effect of the added grid refinement in Grid 2 is dramatically seen again in these time histories. The increases in elevations and velocities are generally more prominent in the southern sites, yet there are exceptions, such as increased velocities in Grays Harbor. The increases in elevations and velocities on Grid 2 can be as large as twice the values computed on Grid 1. The higher frequency components of the waves also are better preserved, thus validating the notion that the Grid 1 resolution caused higher frequencies to be aliased to lower frequencies. Myers and Baptista (1998a, 1998b) further investigate the importance of grid refinement on frequency aliasing, truncation errors, and energy errors.

The elevation and velocity time histories provide a temporal view of what is occurring at specific points, but to gain a spatial awareness of the wave behavior throughout a local area it is instructive to look at isolines of maximum elevations and velocities. The web version of this paper shows these isolines for all of the scenarios in Newport and Seaside and provides analysis of the physical interpretation of these plots. Figure 13 shows the isolines of maximum elevation observed throughout the 1A Grid 1 simulation in Seaside. This area is much more susceptible to inundation than Newport, owing to the generally low topography of the region. The 1A scenario inundates most of the town of Seaside and the valley south of Seaside. The town of Gearhart, just north of the Neawanna River, is inundated through much of the low areas, although there appear to be more potential evacuation routes than Seaside. Much of Seaside is located between the Necanicum River and the coastline and between the Neawanna River and Necanicum River. The "1" scenarios show much of this area to be inundated, although there may be a few spots that could potentially serve as last-option evacuation points (these areas are being resurveyed to ensure that the topography is adequately high at those points). The 1C simulation on Grid 2 indicates the most impact, with essentially all of Seaside experiencing inundation. There are some differences between the 1A and 1C simulations made on the two grids as well. The 1C simulation on Grid 2 showed more inundation than the Grid 1 simulation, most likely owing to the increased grid resolution offshore of Seaside (since the grids are equivalent in Seaside). The 1A simulation on Grid 2 also showed more inundation than the 1A results on Grid 1. The "2" scenarios show less inundation than the "1" scenarios in the Seaside area.

Maximum velocities are also presented and discussed in the web version of this paper. The intensity of the tsunami waves needs to be evaluated in terms of both the potential energy (wave heights) and the kinetic energy (velocities). As tsunami waves surge through coastal waters and inland areas, much of the potential energy may be converted into kinetic energy. Therefore the analysis of maximum velocity magnitudes and directions is critical in assessing the full impact of the waves as they reach land. Analysis of offshore velocities can provide information that may be used to determine where boats at sea should try to find safety. A couple of particle tracking experiments are presented off the coasts of the Columbia River and Yaquina Bay in the web version of the paper.

Another useful tool from a mitigation vantage is to view the arrival times of the first inundating waves. Arrival times in Newport and Seaside are presented for all of the scenarios in the web version of the paper. Most of the scenarios show that much of the inundation in the Newport area occurs during the first 30 or 40 minutes, thus primarily associated with the initial waves. Only the 1A, Grid 1 simulation shows some areas (the northern fringes of the channel and the peninsula next to the marina) to not be

inundated until several hours into the simulation. The tsunami arrival times in Seaside are shown in Figure 14 for the 1A Grid 1 scenario. The waves in the "1" scenarios show that much of the inundation comes from the initial waves overtopping the land from the shoreline. Therefore, the "1" arrival times show an increasing pattern from west to east. The northern fringes of Gearhart in these scenarios witness the waves' arrival an hour or so after the earthquake. The "2" scenarios portray more of a surge of the waves through the estuary and the Necanicum and Neawanna rivers. Much of the inundation in these scenarios is therefore aligned along these waterways.

CONCLUSIONS

Communities in close proximity to the Cascadia Subduction Zone face the task of designing hazard mitigation plans for near-field tsunamis. Modeling past Cascadia events under the constraints of current geologic and geophysical data provides the best indicator as to what could potentially occur in future events. The seismic source scenarios used in this study were based upon a careful selection of deformation modeling techniques and utilization of geophysical, geologic, and thermal information in an effort to minimize uncertainties associated with the initial conditions to the hydrodynamic model.

Simulations of potential Cascadia tsunamis, using the initial conditions from the deformation scenarios, were evaluated from both regional and local perspectives. The regional simulations indicated the importance of bathymetry, coastline geometry, and the varying depths of water in which the deformation is occurring. All of these factors can affect the propagation behavior of the wave as it approaches the shoreline and interacts with the coastline. For example, the Heceta and Perpetua banks off the coast of central Oregon were shown to affect the focusing of waves, exemplified by increased maximum elevations, increased maximum velocities, and changes in the frequencies of the waves. The offshore canyons and banks in northern Oregon and Washington were also shown to incite similar wave behavior. The placement and width of the deformation zone also affects what types of waves will be generated in which areas. For example, off the coast of Washington, the deformation is generally occurring in deeper water, and the width of the locked zone is larger. Therefore, the waves in the north should be larger and have longer wavelengths.

From a local perspective, a city's topography, shoreline geometry, and estuary configuration can each play a critical role in determining the wave behavior as it interacts with the coastline. The local modeling results at the two sites considered in this study, Newport and Seaside, showed a stark contrast in how the waves behaved in areas of such different topographies. Seaside, which is much lower in topography than Newport, was highly susceptible to inundation. Newport, on the other hand, was primarily at risk in the lower regions south of Yaquina Bay. Because the channels leading back to the bay are more maintained and defined than the channels in Seaside, the velocities in the Newport waterways were more significant. The behavior of the waves and the evaluation of inundation risk in each of the simulations was evaluated in several contexts including maximum wave elevations, maximum velocities, maximum velocity vectors, time histories of flow, dominant frequencies, arrival times of the inundating waves, and particle tracking. Each of these tools helps in the assessment of the physical mechanisms of the waves and the likely impact of future tsunamis.

Assessment of the hazards along the coast should bear in mind that although numerical models are tools formulated from governing equations of physics, there are inherent uncertainties tied in to the modeling process that should be adequately identified and, when possible, quantified in its usage. These uncertainties can be classified as seismic source, hydrodynamic model, or data uncertainties. The seismic source uncertainties are the most problematic due to the inability to adequately validate whether the deformation models are reproducing the true deformations of any past subduction events. This leaves far too much freedom in selecting a source. In most cases of modeling the deformation for past events, the computed seismic source is the one which is optimized to produce numerically modeled tsunamis that are the most similar to the tide gauge recordings of the waves. But if there are uncertainties in the

hydrodynamic numerical model, then those errors will be embedded into the seismic source, and ultimately there is no adequate way to verify that source. The approach taken in this study was to derive a source using an advanced deformation model with as much available geophysical data as input, and to not rely on the use of a hydrodynamic model in determining the source. We were thus trying to constrain the errors in the deformation model as best possible, without embedding any other (i.e. hydrodynamic model) errors into the source.

These other errors are present, as exemplified by the differences in results on the two grids used in this study. Such uncertainties in the hydrodynamic model can be associated with energy preservation, underlying assumptions in the shallow water equations, numerical diffusion, and truncation errors. Each of these errors is dependent upon other factors such as grid refinement and parameter selection, as discussed in more detail in Myers and Baptista (1998a-b). Errors may also be present in the models due to data uncertainties. For example, the model's representation of the bathymetry and topography will always carry uncertainties in how well the geoid shape is reproduced. Many of these uncertainties can be minimized by increasing the grid refinement. However, this study used grids that had $8\text{-}10x10^4$ nodes, thus requiring the use of time steps on the order of a tenth of a second. Therefore, simulations on such grids are computationally intensive, and any further refinement needs to be carefully placed. These issues are further discussed in Myers and Baptista (1998a, 1998b) in an effort to quantify the performance of tsunami simulations.

ACKNOWLEDGMENTS

We thank Rick Luettich and Joannes Westerink for providing the base code for ADCIRC. This research was partially sponsored by DOGAMI Contracts 411001 and 6175001, NEHRP Award 1434-HQ-96-GR-02712, Department of Defense Army Research Office Grant DAALO3-92-G-0065, and Oregon Sea Grant No. N00014-96-1-0893.

REFERENCES

Atwater, B.F., Nelson, A.R., Clague, J.J., Carver, G.A., Yamaguchi, D.K., Bobrowsky, P.T., Bourgeois, J., Darienzo, M.E., Grant, W.C., Hemphill-Haley, E., Kelsey, H.M., Jacoby, G.C., Nishenko, S.P., Palmer, S.P., Peterson, C.D., and Reinhart, M.A., 1995, Summary of Coastal Geologic Evidence for Past Great Earthquakes at the Cascadia Subduction Zone, *Earthquake Spectra*, 11(1), 1-18.

Baptista, A.M., Priest, G.R., and Murty, T.S., 1993, Field Survey of the 1992 Nicaragua Tsunami, *Marine Geodesy*, 16(2), 169-203.

Committee on the Alaska Earthquake of the Division of Earth Sciences National Research Council, 1972, *The Great Alaska Earthquake of 1964*, Oceanography and Coastal Engineering, National Academy of Sciences, Washington, D.C.

DeMets, C., Gordon, R.G., Argus,D.F., and Stein, S., 1990, Current Plate Motions, *Geophysical Journal International*, 101(2), 425-478.

Flück, P. Hyndman, R.D., and Wang, K., 1997, Three-Dimensional Dislocation Model for Great Earthquakes of the Cascadia Subduction Zone, *Journal of Geophysical Research*, 102(B9), 20539-20550.

Fukao, Y., Tsunami Earthquakes and Subduction Processes Near Deep-Sea Trenches, 1979, *Journal of Geophysical Research*, 84(B5), 2303-2314.

Geist, E. and Yoshioka, S., 1996, Source Parameters Controlling the Generation and Propagation of Potential Local Tsunamis Along the Cascadia Margin, *Natural Hazards*, 13(2), 151-177.

Goldfinger, C., 1996, personal communication, Oregon State University.

Hebenstreit, G.T. and Murty, T.S., 1989, Tsunami Amplitudes from Local Earthquakes in the Pacific Northwest Region of North America Part 1: The Outer Coast, *Marine Geodesy*, 13(2), 101-146.

Holdahl, S.R. and J. Sauber, 1994, Coseismic Slip in the 1964 Prince William Sound Earthquake: A New Geodetic Inversion, *Pure and Applied Geophysics*, 142(1), 55-82.

Horning, T., 1997, personal communication, Cannon Beach.

Hyndman and Wang, 1993, Thermal Constraints on the Zone of Major Thrust Earthquake Failure: The Cascadia Subduction Zone, *Journal of Geophysical Research*, 98(B2), 2039-2060.

Hyndman and Wang, 1995, The Rupture Zone of Cascadia Great Earthquakes from Current Deformation and the Thermal Regime, *Journal of Geophysical Research*, 100(B11), 22133-22154.

Kanamori, H., 1996, personal communication, California Institute of Technology.

Lander, J.L. and Lockridge, P.A., 1989, *United States Tsunamis*, National Geophysical Data Center, Publication 41-2.

Lander, J.L., Lockridge, P.A., and Kozuch, M.J., 1993, *Tsunamis Affecting the West Coast of the United States*, National Geophysical Data Center, Documentation No. 29.

Luettich, R.A. and Westerink, J.J., 1995a, *An Assessment of Flooding and Drying Techniques for Use in the ADCIRC Hydrodynamic Model: Implementation and Performance in One-Dimensional Flows*, Dept. of the Army, U.S. Army Corps of Engineers, Vicksburg, MS.

Luettich, R.A. and Westerink, J.J., 1995b, *Implementation and Testing of Elemental Flooding and Drying in the ADCIRC Hydrodynamic Model*, Dept. of the Army, U.S. Army Corps of Engineers, Vicksburg, MS.

Luettich, R.A., Westerink, J.J., and Scheffner, N.W., 1991, *An Advanced Three-dimensional Circulation Model for Shelves, Coasts, and Estuaries*, Dept. of the Army, U.S. Army Corps of Engineers, Washington, D.C.

Mansinha, L. and Smylie, D.E., 1971, The Displacement Fields of Inclined Faults, *Bulletin of the Seismological Society of America*, 61(5), 1433-1440.

Myers, E.P. and Baptista, A.M., 1995, Finite Element Modeling of the July 12, 1993 Hokkaido Nansei-Oki Tsunami, *Pure and Applied Geophysics*, 144 (3/4), 769-801.

Myers, E.P. and Baptista, A.M., 1998a, Modeling of Past Tsunamis: One Model's Lessons from the 1993 Hokkaido Nansei-Oki and 1964 Alaska Tsunamis, (submitted to *Natural Hazards*).

Myers, E.P. and Baptista, A.M., 1998b, Numerical Considerations in Finite Element Simulations of Tsunamis, (submitted to *International Journal for Numerical Methods in Fluids*).

Ng, M.K.-F., Leblond, P.H., and Murty, T.S., 1990, Simulation of Tsunamis from Great Earthquakes on the Cascadia Subduction Zone, *Science*, 250, 1248-1251.

Nunez, R. 1990, *Prediction of Tidal Propagation and Circulation in Chilean Inland Seas Using a Frequency-Domain Mode*, Master of Science Thesis, Oregon State University.

Okada, Y., 1985, Surface Deformation due to Shear and Tensile Faults in a Half-Space, *Bulletin of the Seismological Society of America*, 75(4), 1135-1154.

Priest, G.R., 1995, *Explanation of Mapping Methods and Use of the Tsunami Hazard Maps of the Oregon Coast*, State of Oregon, Department of Geology and Mineral Industries, Report O-95-67, 95 p.

Priest, G.R., Myers, E.P., Baptista, A.M., Flück, P., Wang, K., Goldfinger, C., 1997, Fault Dislocation Scenarios for a Tsunami Hazard Analysis of the Cascadia Subduction Zone (in preparation).

Tadepalli, S. and Synolakis, C.E., 1994, The Run-up of N-waves on Sloping Beaches, *Proceedings of the Royal Society of London A*, 445, 99-112.

Turner, P.J. and Baptista, A.M., 1991, *ACE/gredit Users Manual: Software for Semi-automatic Generation of Two-Dimensional Finite Element Grids*, CCALMR Software Report SDS2(91-2), Oregon Graduate Institute of Science & Technology, Portland, OR.

Visher, P., 1998, personal communication, Cannon Beach, Oregon.

Whitmore, P.M., 1993, Expected Tsunami Amplitudes and Currents Along the North American Coast for Cascadia Subduction Zone Earthquakes, *Natural Hazards*, 8(1), 59-73.

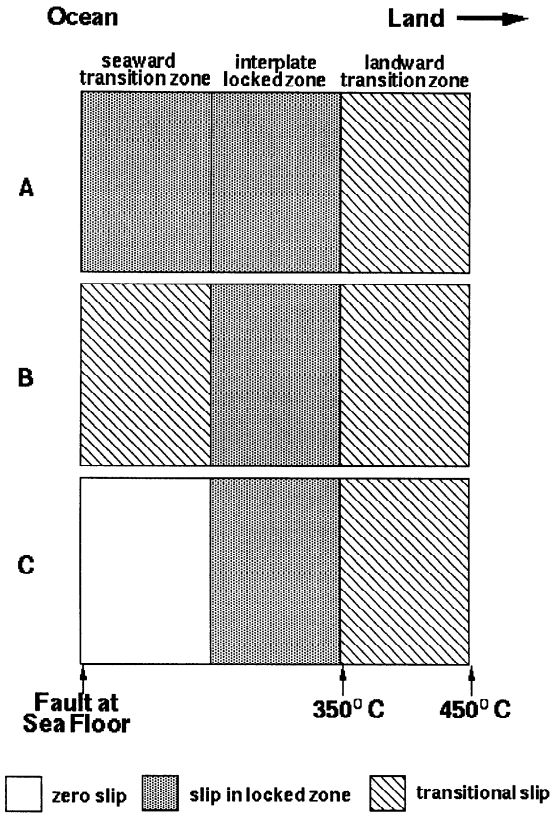

Figure 1. Distribution of slip for the three scenarios.

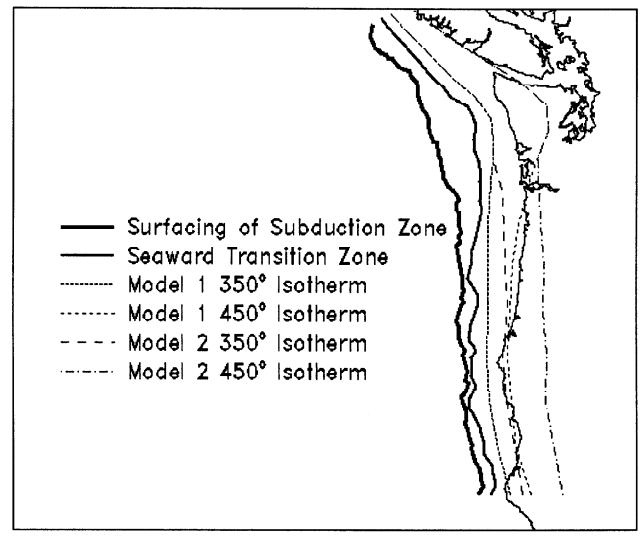

Figure 2. Positions of slip distribution zones.

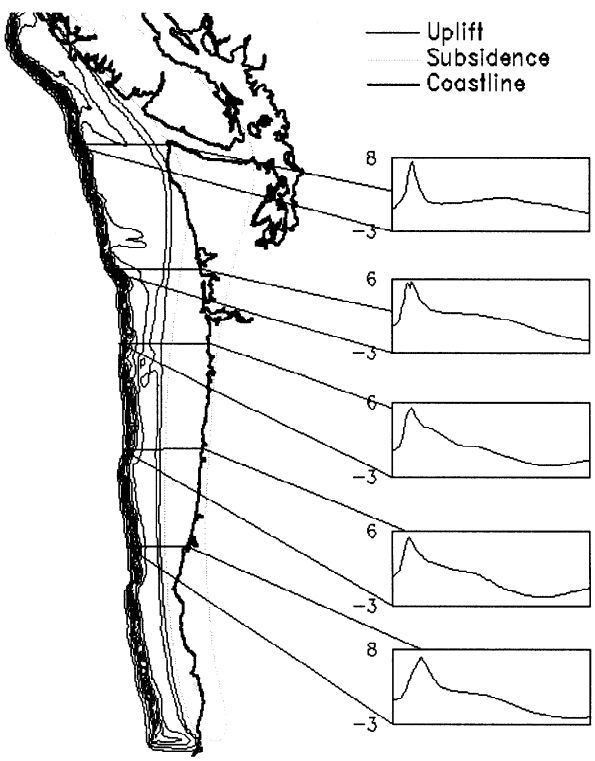

Figure 3. Deformation for scenario 1A.

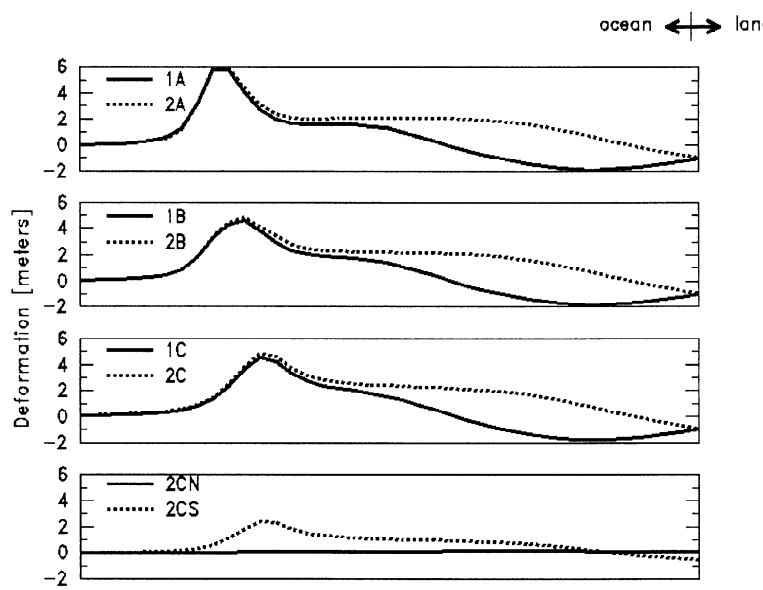

Figure 4a. Cross section of deformations offshore of Newport, OR.

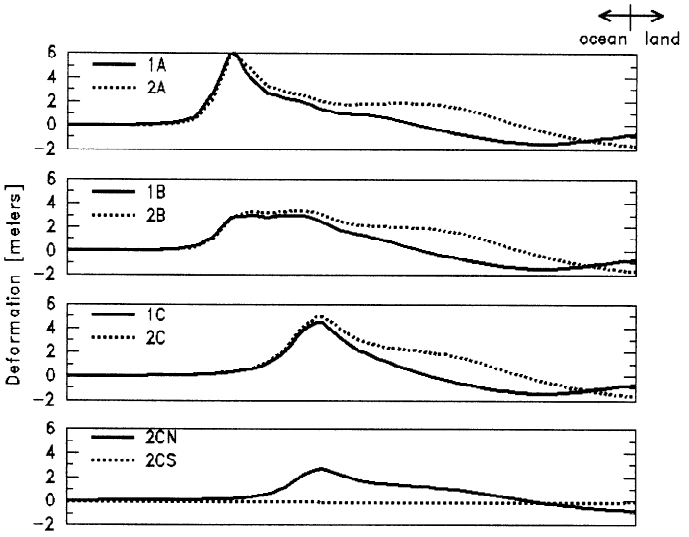

Figure 4b. Cross section of deformations offshore of Seaside, OR.

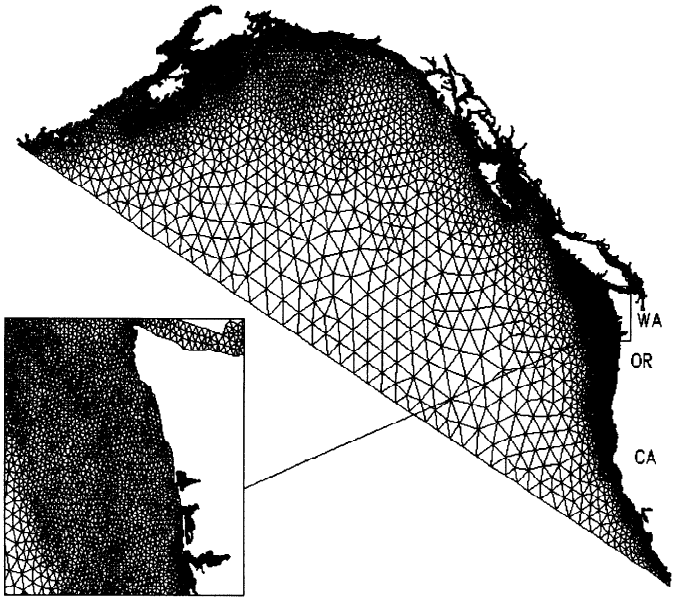

Figure 5a. Finite element grid 1.

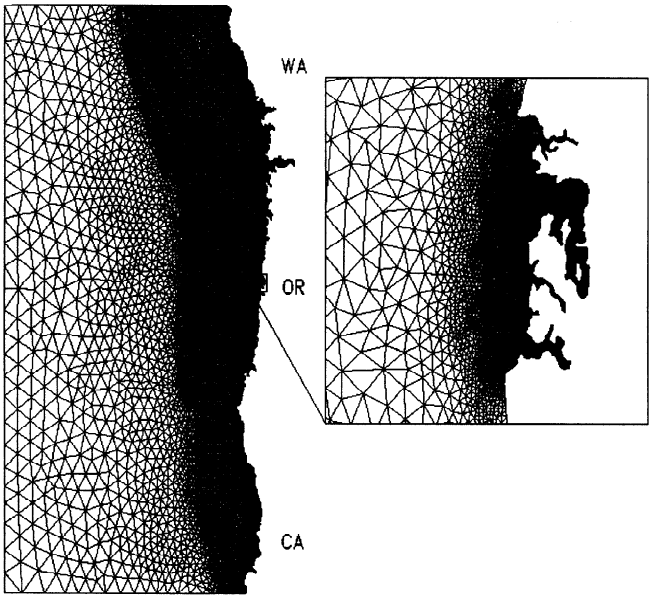

Figure 5b. Finite element grid 2.

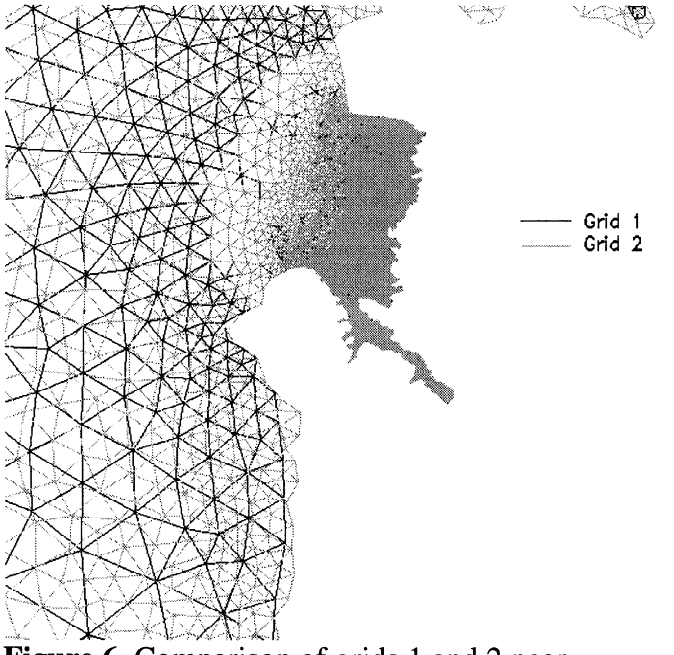

Figure 6. Comparison of grids 1 and 2 near Seaside, OR.

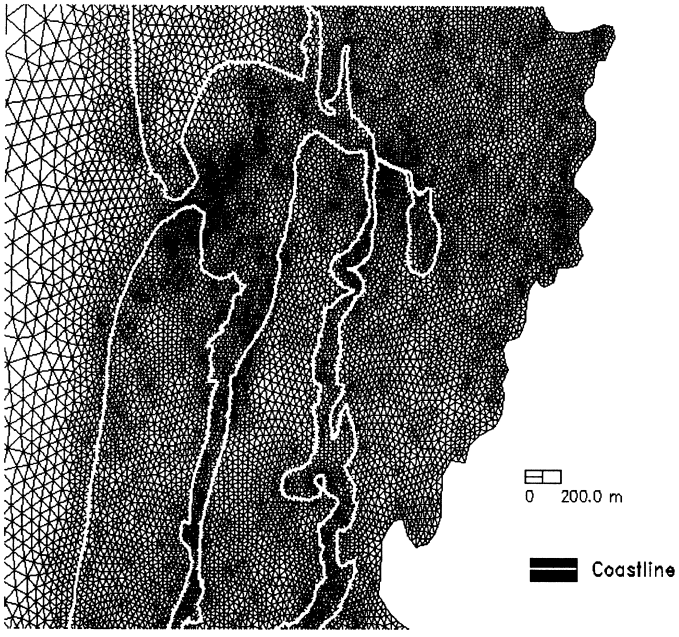

Figure 7a. Grid refinement in Seaside, OR.

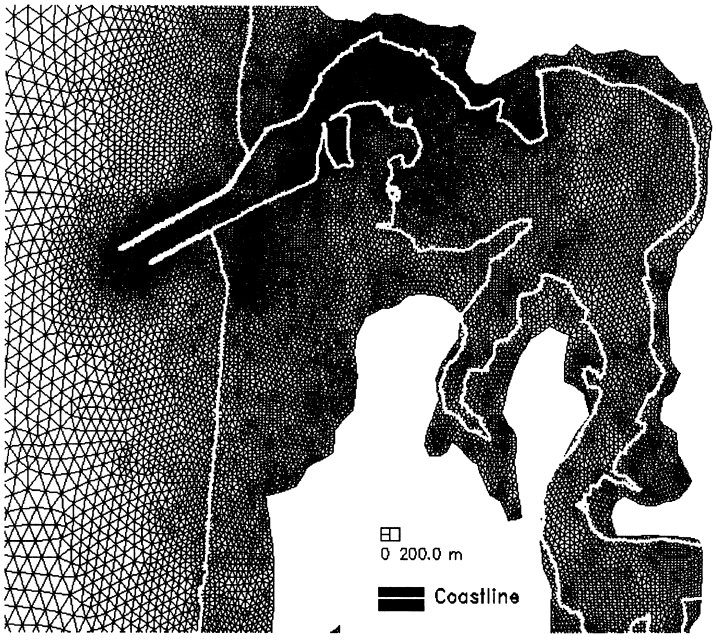

Figure 7b. Grid refinement in Newport, OR.

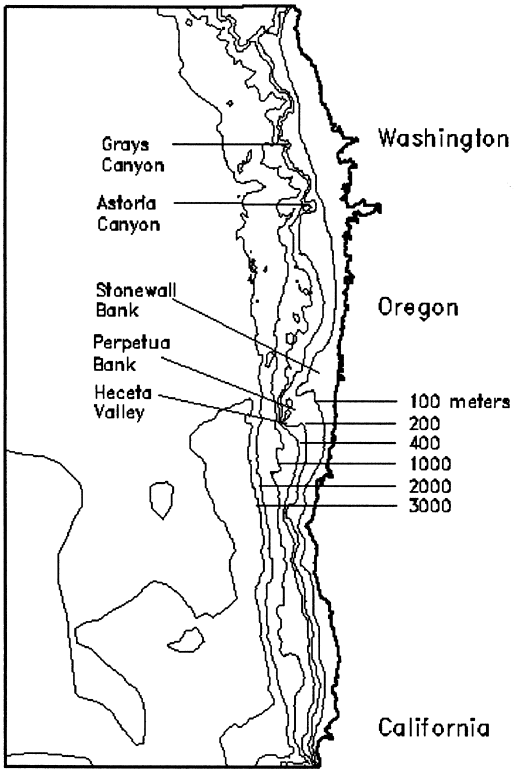

Figure 8. Bathymetry throughout the domain.

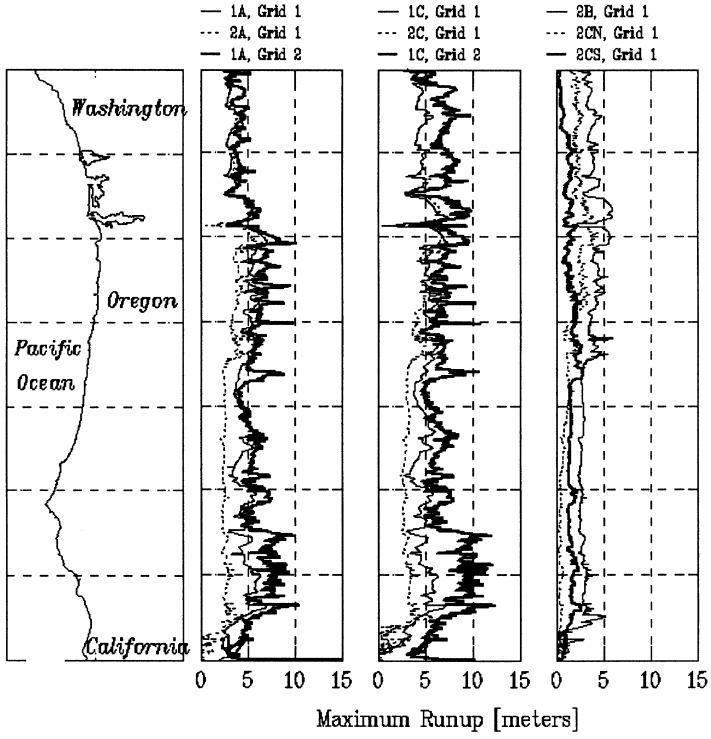

Figure 9. Maximum coastal wave elevations.

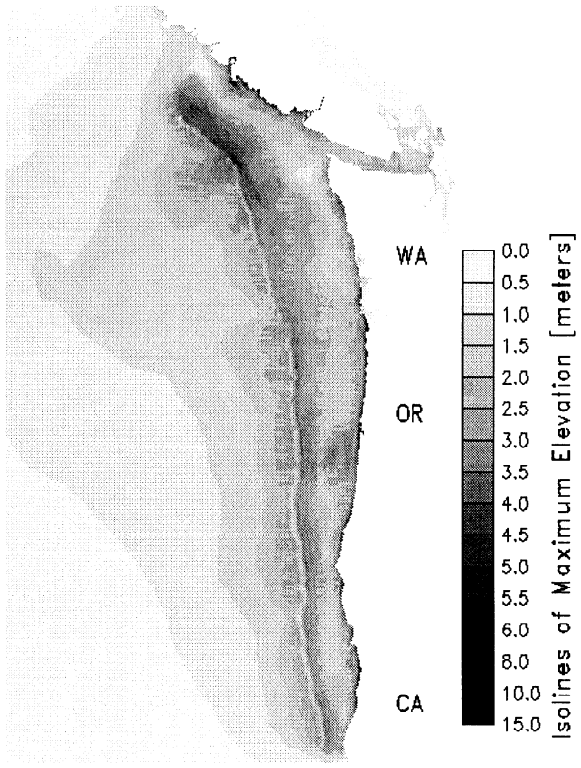

Figure 10. Isolines of maximum elevation for scenario 1A.

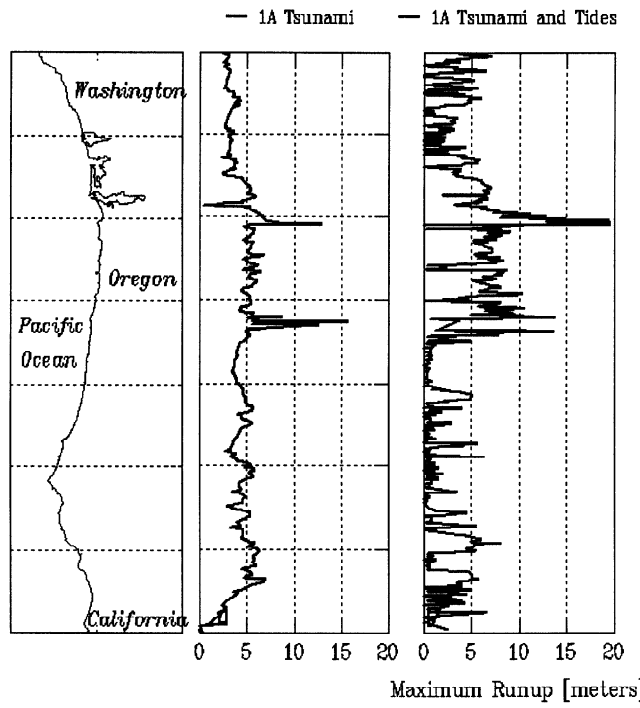

Figure 11. Maximum coastal wave elevations with the inclusion of tidal forcing during the 1A grid 1 simulation.

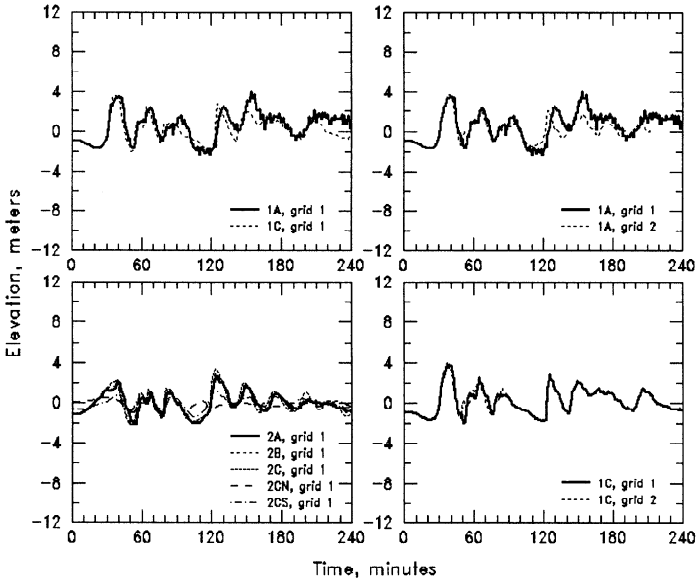

Figure 12a. Elevation time histories near the entrance of Yaquina Bay, OR.

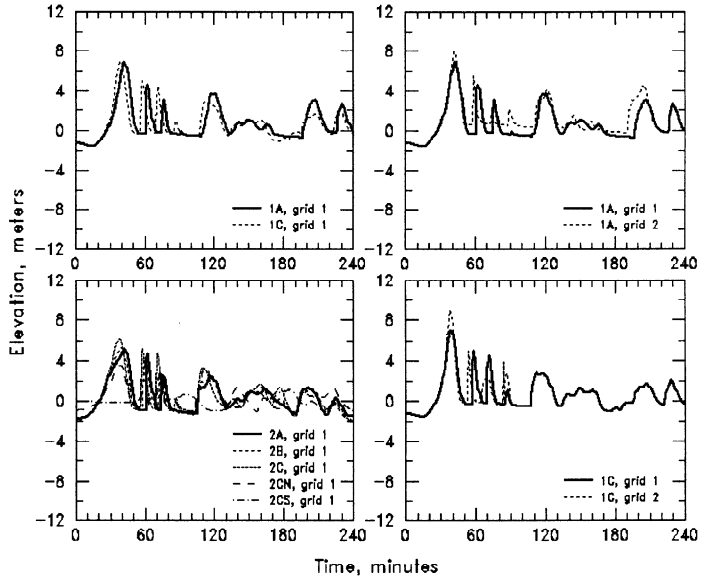

Figure 12b. Elevation time histories near Seaside, OR.

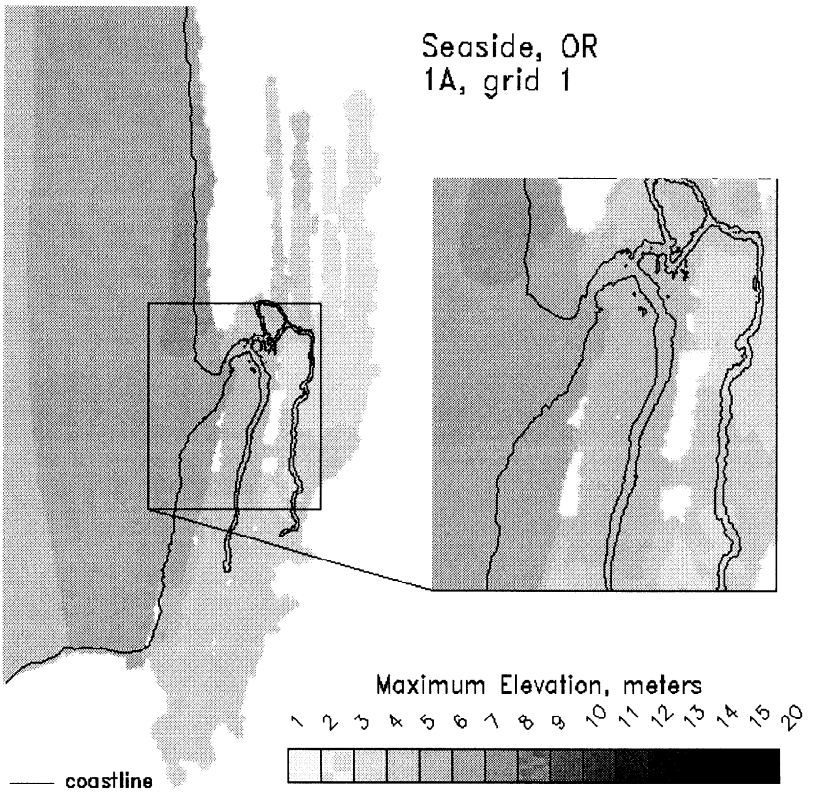

Figure 13. Isolines of maximum elevation near Seaside, OR for 1A, grid 1.

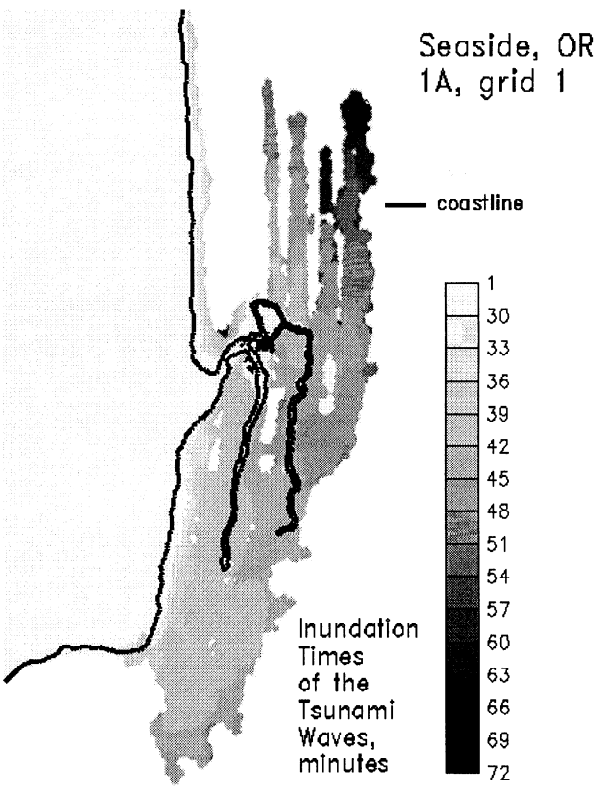

Figure 14. Tsunami arrival times near Seaside, OR for 1A, grid 1.

ANATOMY OF A LANDSLIDE-CREATED TSUNAMI AT SKAGWAY, ALASKA November 3, 1994

Bruce A. Campbell, P.E.
Consulting Engineer
14104 Hancock Drive
Anchorage, Alaska 99515
907-345-3129

&

Dennis Nottingham, P.E.
Peratrovich, Nottingham & Drage, Inc.
1506 West 36th Avenue
Anchorage, Alaska 99503
907-561-1011

ABSTRACT

At 7:10 p.m. on November 3, 1994, a large tsunami generated by a massive landslide in the submerged Skagway River delta occurred near Skagway, Alaska, resulting in one fatality and damaging or destroying many harbor structures.

At first, it was theorized by some that construction activity in the harbor caused the initial landslide. However, this paper presents the findings of an in-depth scientific investigation that concludes that such a theory is impossible.

The findings paint a clear picture of the failure of the submerged Skagway River delta that was overloaded by flood sediments and exacerbated by river diking. Slide volumes estimated at over 20,000,000 cubic yards that consisted of a massive initial slide and subsequent retrogressive earth slides produced the tsunami that caused the fatality and destroyed or damaged harbor structures.

The analysis relies on physical evidence and reconstructs the tsunami on a second-by-second time-line that shows conclusively that the failure of the submerged Skagway River delta was not caused by the harbor construction. Each shred of evidence is examined and the event systematically reconstructed on a step-by-step basis without interjecting supposition, speculation, theory or hypotheses.

PREFACE

The post-mortem of the Skagway tsunami that occurred on November 3, 1994, was not achieved all at once, but was performed in stages over a period of about four years.

Basically, the post-mortem of the Skagway tsunami can be separated into three categories.

1) An initial investigation that occurred in late 1994 and early 1995. This phase was concerned only with determining if the cause of the tsunami was in any way related to the construction activity that was in progress at the Pacific and Arctic Railway and Navigation Co. (PARN) dock on the east side of the harbor (Figure 1). This culminated in a report dated January 16, 1995, which was the first analysis published(1). The report concluded that, based on eyewitness observations and physical evidence, construction activity was not the cause of the tsunami.

2) The legal phase next occurred. Reports by other investigators identified the PARN dock construction activity as the sole cause of the tsunami. These reports, issued primarily in 1995, were in response to requests by various attorneys involved in lawsuits concerning the event. These other findings were, in many cases, in total disagreement with the conclusions contained in the January 16, 1995, analysis. This instigated a more detailed investigation of not only the role played by the construction activity, if any, but to categorically determine the anatomy of the underwater landslide and resulting tsunami. This phase occurred in 1995 – 1997.

3) The third phase, which has been coined the confirmation phase, occurred basically in 1998. This phase consisted primarily of underwater observations and measurements that confirmed previous determinations as to locations and sequences of the various segments of the initial delta landslide and subsequent retrogressive and subaerial slides which spawned the tsunami.

It is the purpose of this publication to integrate the three phases into a comprehensive report that will not only provide future investigators with details of the anatomy of the Skagway River delta landslide and resultant tsunami, which occurred on November 3, 1994, but will highlight the need for a scientific-based tsunami warning system.

TAIYA INLET TSUNAMI

Skagway, Alaska, is located near the head of Taiya Inlet, a narrow fjord where the Alaska Panhandle joins the interior of the state. The fjord is approximately 15 miles long, averages slightly less than a mile wide and is flanked on either side by mountains rising to 7,000-foot elevations within 10 miles of the inlet. The fjord itself has a maximum depth of about 1,400 feet and has very abrupt, steep side slopes. The tidal range in the inlet is about 27 feet—from a –5' mean lower low water (MLLW) to a +22' MLLW.

Two rivers feed the inlet—the Taiya River at Dyea and the Skagway River at Skagway. Since both head in rugged, mountainous, glacier areas they have steep gradients, carry substantial suspended sediment loads, and transport large bed loads consisting of gravel or larger material during periods of high water. The Skagway River gradient averages over 4 percent, dropping nearly 3,000 feet in 13 miles.

Pacific storms abound and heavy local rainfalls are experienced as the moisture-laden, eastward-flowing pacific air collides with the coastal mountains in the Skagway area.

Skagway is constructed on the upland portion of the Skagway River delta and occupies nearly the entire delta area, leaving only a minimal channel for the river on the western side of the delta. (Figure 1).

Since Skagway was founded, in 1898, a concerted effort has been sustained to prevent the river from traversing its upland delta, as it would normally do without man-made constraints. Dikes have been constructed by both the U.S. Corps of Engineers and the White Pass and Yukon Railroad, assisted to a lesser degree by the City of Skagway and the State of Alaska.

The intertidal face of the original delta has been modified by the addition of several water-oriented developments. These facilities, coupled with the upriver dikes, restrict the present river to a much lesser delta deposition area than it originally enjoyed.

Extension by the State of the airport runway into the intertidal area of the delta in about 1973, further restricted the river's deposition area by creating a flow diversion that now directs the river even farther to the west.

As a direct result of man's intervention, the Skagway River's original delta face of about 3,000 feet is now confined to about 500 feet. This restriction to a river carrying a large suspended load and moving a huge bed load at high water has caused a major change in the natural deposition pattern and created a much narrower delta which is now directed across Taiya Inlet, instead of down the Inlet.

The consequences of the river delta being changed by intertidal development were first alluded to in a 1972 U.S.G.S. paper(9). This paper, authored by Lemke & Yehle, was the result of a hazard study performed in response to the infamous 1964 Alaska earthquake that produced a tsunami that caused widespread damage throughout the Gulf of Alaska.

Records indicate that at least three sizable tsunamis have occurred previously in Taiya Inlet in recent times. These were in 1899, 1958, and 1994. The third is the subject of this analysis. It occurred at about 7:10 p.m. on November 3, 1994, (local time). In addition numerous smaller tsunamis have also been recorded or noted.

Setting the Stage

Southeast Alaska (the Panhandle) is noted for its stormy weather which includes frequent precipitation and strong winds. Storms from the southeast bring driving rains and/or snow riding on winds that are frequently in excess of 50 mph. The fjord topography tends to channel the winds and, in many cases, accelerates them.

During the first week in October 1994, a severe storm attacked the Skagway area. The intense rainfall that occurred caused the Skagway River to flood to a record or near record level.

Stan Selmer was at that time the Mayor of Skagway. In a town of roughly 600 permanent residents, the mayor has a lot of extraneous duties. One of Stan's duties was to monitor flood flows in the Skagway River and to alert his fellow citizens when it was time to evacuate.

During the very early morning of October 4, 1994, the river crested at, or near, record height. Since this occurred in early morning darkness, photographic recordings were not possible. Several residences were evacuated and flood alerts given. At first light in the morning, Stan took a video recording of the flood, which, by that time (6 hours later), had diminished about 4 feet in height according to Stan's observation. The video shows a raging water flow with an obvious heavy suspended load. From the noise it can be concluded that a sizable bed load is moving downstream and onto the subaqueous delta.

This major flooding occurred only about a month before the delta landslide and tsunami occurred in Taiya Inlet. Obviously, this major flood dumped a considerable amount of both suspended and bed load debris on the subaqueous delta of the Skagway River. The amount of debris cannot be rationally determined, but it is safe to say that probably several million tons of debris was carried into the delta area by the raging flood.

During this October-November period, a construction project was underway at the PARN dock (Figure 1). The work consisted of removing a portion of the old wood dock and replacing it with open steel sheet pile cells. The contractor (Sandstrom & Sons) was working a double shift: 7:00 a.m. to 5:00 p.m. and 7:00 p.m. to 5:00 a.m. Rock armor for later use in the project was being hauled to the site by the White Pass and Yukon Railroad (now owned by PARN) and stockpiled adjacent to the construction area between the railroad and the dock (Figure 2).

On November 3, 1994, the construction crew night shift was preparing to go to work. It was raining (with some snow) and the wind was blowing at an estimated speed of 25 mph up the inlet toward Skagway. It was dark. A very low tide of nearly –5' MLLW occurred about this time (one of the lowest of the year).

The Event

At approximately 7:10 p.m. a tsunami occurred with an amplitude of approximately 30 feet at the construction site. There were four eyewitnesses who observed the tsunami at the work site—all were Sandstrom and Sons employees. A fifth witness was on a boat in the small boat harbor and did not see the tsunami, but he felt the effects when his boat hit the bottom of the harbor. Figure 2 shows the general layout of the work site just before 7:10 p.m. on November 3, 1994.

The eyewitnesses reported the following occurrences. Many of their observations were not reported initially in police reports, but were brought to light in later interviews in answer to specific queries.

1) As the crew prepared to start work, two members, Taylor and Garoutte, reported that the 25-mph southeast driving wind suddenly diminished to a calm. The crane operator (Kirk Garoutte) later reported that the sudden change in weather, from a rain-laden driving wind to a calm, still condition, was "spooky."

2) Bill Armstrong was on a boat in the small boat harbor when he felt a shock, like a wind surge followed by the boat hitting bottom.

3) About a minute later two of the eyewitnesses, Bill Taylor (superintendent) and Karl Wallin (foreman), reported that the newly-installed steel sheet piles in the unfilled 4½ completed cells "rattled" and "snapped."

4) Taylor reported that the sheet piles seemed to lean. The crane operator (Garoutte) reported that he thought his crane was rotating, but when he hit the swing brake and there was no sudden jolt he realized that his crane was not rotating, but that the cells and everything within his field of view was very slowly moving seaward.

5) Taylor turned to shout a warning to the two workers in Cell #5 (Jack Young and Paul Wallin). When he turned back, the sheet piles were gone and a large wave was coming directly toward him along the dock axis and was within the area where the cells had been. He observed a section of the old wooden south dock with a portable metal gangway on it riding on the wave crest. The foreman, K. Wallin, reported that the large wave coming up the old dock axis toward him appeared to overtop the sheet piles just as they disappeared. He also reported that a section of the wooden south dock with something shiny on it was riding on the wave crest.

6) K. Wallin next saw his brother (P. Wallin) engulfed with water and debris within Cell #5. Taylor saw a D-7 Cat tractor, which was parked behind Cell #4, tilt. He then turned and ran. Garoutte saw the D-7 Cat tilt, stop, and then roll into the water. He then also ran.

7) Taylor saw the blue work barge above the bull rail of the old dock as he ran northerly. (This observation provided data from which it was possible to determine the approximate tsunami elevation at the construction site.)

8) About the time Garoutte stopped running, he heard a large crashing noise in the general direction of the ferry terminal and also observed the lights on the ferry terminal disappear as something blocked his line of vision. He speculated that it was a wave.

9) Garoutte returned to the crane, observed a section of the old wooden south dock with the gangway on it floating about where Cells #4 and #5 had been.

10) Stan Selmer, Mayor of Skagway, arrived at the small boat harbor about 4 minutes after the tsunami passed the construction site and found the small boat harbor entrance plugged solid with old dock debris which prevented a search boat from leaving the harbor. The next morning, Stan was at the ferry terminal site and observed that a portion of the rock stockpile remained at the construction site where it had been stockpiled. The distance between the ferry terminal and the stockpile site was roughly ¼ mile.

The Evidence

To be valid, any analysis to determine the cause of this tsunami must be consistent with all the facts and evidence. If any finding is in contrast to any of the known facts or evidence it cannot be correct. Speculation, theory and hypothesis have no place in failure investigations.

The purpose of this post-mortem is to assemble all the evidence and facts that exist and use them to accurately define the anatomy of this event.

The observations by the eyewitnesses are the prime evidence of what actually occurred, the sequence of events, and the timing of those events.

The National Oceanic and Atmospheric Administration (NOAA) has maintained a tide gage within the Skagway Harbor area for several years. This gage, of course, was designed to respond to only long period waves (tides). The period of the November 3, 1994, tsunami was, however, of sufficient length to be recorded by the NOAA tide gage, but in a damped format. The tide gage trace added another piece of evidence for use in the post-mortem performed to determine the specific details of the slide that caused the tsunami. (Figure 3).

As is the case in most construction projects, photographs were taken during the rebuilding activity on the PARN dock. On the morning following the event (November 4, 1994), more photographs were taken by various persons, including Jeff Brady of the Skagway News, and local photographer Gary Heger. Several persons, among them Mayor Stan Selmer, reported the conditions that were observed at first light the next morning.

Three days after the event the engineer for the construction project, Peratrovich, Nottingham, and Drage, Inc. (PN&D), began a detailed sounding of Taiya Inlet using GPS (ground positioning system) and a continuous recording sonar depth gage. Soundings required about two days to complete—November 7^{th} – 9^{th}. These data were vital evidence to be considered in the post-mortem.

Since each failure is unique, reconstruction of the event on a step-by-step basis depends on evidence specific to the particular failure event.

The final determination as to the cause of the Skagway tsunami must be consistent with every piece of evidence. If it is not, then either the determination of cause is wrong or the evidence is not valid and must be so proven. It's one or the other—there is no in-between.

The initial concern was: "Did the construction at the PARN dock cause the tsunami?" Construction projects are referenced as causes or "triggers" in much of the literature concerning landslides and resulting tsunamis in fjords. A review of literature failed to uncover a single incident of actual

evidence that construction activity triggered an underwater slide and tsunami—a lot of assumptions, speculations, and hypotheses, but not a shred of evidence or proof.

The 1995 investigation and subsequent reports of the event were targeted solely to this single issue(2)(3)(4). Eyewitness observations were initially recorded in police reports, which were hurriedly taken at approximately 9:20 p.m. on November 3, 1994. Interviewing the eyewitnesses to ascertain more details of the event was a number one priority of the second stage of the investigation. As a result of initial interviews in January 1995, it was ascertained that the tsunami traveled up the old south dock directly toward the work site, where three of the eyewitnesses were located. Their location, especially elevation, put them in a position to achieve a good overview of the whole situation. The fourth witness, Jack Young, was on the ground in cell #5 and had only a very restricted field of view.

The eyewitnesses reported that the initial wave crest "seemed to overtop the sheet piles just as they disappeared," and carried a portion of the old south dock wooden deck with a portable metal gangway on it. The wave did not overtop the old north dock, but the blue work barge that was tied up to the north dock was visible above the dock bull rail. Since the elevations of the sheet pile that were overtopped is known and the north dock elevation is also known, as well as the geometrics of the barge, a rational tsunami amplitude elevation at the construction site can be computed within an acceptable tolerance.

Before and after photos taken by Heger and Brady determined the location of the gangway prior to and after the event. Heger's "before" photo shows the gangway stored on the easterly side of the old south wooden dock, about 650 feet south of Cell #1 of the new dock construction, and about 850 feet south of where the three eyewitnesses stood.

The Initial Analysis

These eyewitness accounts, photos, bathymetry, and physical measurements were prime evidence. This evidence supported several conclusions.

Since eyewitnesses reported that the sheet pile "rattled and snapped" before any movement occurred at the construction site and before the wave was observed, common sense tells us that something remote from the immediate site had occurred that caused ground vibrations sufficient to cause the sheet piles to "rattle and snap."

Since the wave was visible at about the same time the sheet pile cells disappeared, the wave could not have originated at the construction site.

The initial wave carried a section of the old south wooden dock with the metal gangway on it. It must therefore be concluded that the south dock was destroyed at some point in time prior to the arrival of the wave at the construction site, since the metal gangway was stored roughly 650 feet south of the construction site where the eyewitnesses observed it riding on the tsunami crest.

The work barge was visible as one of the eyewitnesses (Taylor) ran off the old north dock. Since the dimensions and draft of the barge were known, an estimate within narrow limits, as to the crest elevation of the tsunami that elevated the barge could be calculated. Computations show that the tsunami crest elevation was approximately +25' MLLW. This can be confirmed by observations of the eyewitnesses that the tsunami appeared to "overtop" the sheet pile cells elevation, but did not reach the north dock deck elevation of 29' MLLW. Since the tide was at about –5' MLLW at the time, the tsunami amplitude was about 30 feet at the site.

A tsunami propagates in a circular manner from the point of the disturbance that caused the wave (unless an obstacle of some sort deflects the wave path). The approximate location of the disturbance can hence be determined from the eyewitness observations and physical dimensions.

The tsunami destroyed the old south dock and in the process a section of the wooden deck with gangway aboard floated on the wave crest and traveled about 650 feet from its original location to where the eyewitnesses saw it coming directly at them. The travel path of the deck section with its gangway passenger established the wave direction as being approximately coincident with the old south dock axis. When the travel axis is extended, it should logically pass through the point of origin of the tsunami since no obstructions exist in Taiya Inlet to deflect it. This physical evidence hence established the direction of the epicenter.

The bathymetry of Taiya Inlet procured by PN&D in early November 1994 disclosed a major landslide scarp located between about 4,000 feet to 6,000 feet from the end of the old south dock. This landslide scarp was consistent with the wave direction as established above, and was the only possible source of a landslide of sufficient size to cause a tsunami with an amplitude of about 30 feet at the construction site.

The initial report issued on January 16, 1995(1) based on evidence available at that time, concluded that the event did not start at the construction site, and that the landslide which caused the tsunami occurred about 4,000 feet to 6,000 feet from the end of the south dock on a line approximately coincident with the extension of the old PARN dock axis. The eyewitness reports and physical evidence are conclusive that the event could not have originated at the construction site.

The Second (Legal) Stage

After the initial analysis was issued in January 1995, several lawsuits were filed naming various parties. These lawsuits generally were directed toward establishing fault and liability. The lawyers involved retained various individuals and firms to prepare findings as to the cause(s) to help support their particular lawsuit. Several investigative reports were issued during this period. For the most part these reports all assigned blame for the event to one of the named parties generally in concert with the position of the lawyer who employed the author. Most of these reports were inconsistent with the initial January 1995 report and concluded that the tsunami source was in fact located at the construction site in spite of the eyewitness reports and physical evidence that appeared to be absolutely conclusive that the tsunami did not originate at the construction site. In light of these divergent opinions, which were based primarily on theory, speculation and hypothesis and not on evidence, it was deemed necessary to completely reevaluate the evidence to make certain that the conclusions contained in the January 1995 report were correct. As mentioned above, evidence is primary and always must take precedence over theory, speculation and hypotheses.

The initial step in the reevaluation was to further interview eyewitnesses. A considerable amount of additional information not previously recorded was obtained. All of the new information was totally consistent with previous eyewitness accounts, as recorded in the police reports and/or garnered in the January 1995 interviews with Karl Wallin and Bill Taylor. Several important details emerged.

Bill Taylor remembered that as he walked onto the dock that night the southeast wind all of a sudden died and it became calm. Later, as he turned to run off the dock, he saw the D-7 Cat tilt (it was parked roughly behind Cell #1). As he started his run he noticed that the blue work barge was visible above the old north dock bull rail. When he got in his pickup he looked at his watch—it was 7:12 p.m. (also recorded in his police report).

Kirk Garoutte (crane operator) also recalled the sudden dying of the wind and the calm that followed just before the event. He referred to it as "spooky."

Kirk also recalled that his first inkling of the event came when he thought his crane was rotating and he hit the swing brake and no sudden jolt resulted. He then realized that the crane was not rotating and everything in his field of view was moving very slowly toward the bay. Kirk next stated that the sheet pile cells dropped out of sight just as a wall of water rushed in. As Kirk jumped out of the

crane cab, he also saw the D-7 tractor tilt, stop, and then roll into the water. He raced down the north dock. Karl Wallin reported that his brother Paul in cell #5 disappeared as a huge wall of water and debris crashed over him.

Stan Selmer, Mayor of Skagway, was interviewed and a copy of his October 4th Skagway River flood video reviewed.

Armed with this additional data, a reanalysis was conducted geared not only as to whether or not the event started at the construction site, but to determine exactly where it did start; and to determine the sequence of the various elements of the event of which there were obviously many.

Times were assigned to various occurrences based on the eyewitness reports. The approximate timings were created to put the various elements in proper order and in a relative time sequence.

No.	Approx. Time	Event	Witness
1	-60 to -120 Sec.	Wind stopped; it became calm and quiet at the work site	Taylor/Garoutte
2	0-2 Sec.	Sheet piles rattle and snap	Taylor/K. Wallin
		Sensation of crane moving	Garoutte
3	2-3 Sec.	Old dock sheet piles start to slide seaward Sheet piles start to collapse	Garoutte K. Wallin
		South old dock & sheet piles start to slide away	Taylor
4	3-4 Sec.	Taylor shouts warning	Taylor
		Young scrambles up the bank	K. Wallin
		Young moves toward north old dock and grabs wood pile	Young
5	4 Sec.	P. Wallin hit with falling wood pile	K. Wallin
6	4-5 Sec.	Taylor turned back from shouting a warning and the sheet piles were gone. Saw an incoming wall of water, which carried a section of the old south dock deck with a galvanized metal gangway on it in the area where the cells had been, turned and started to run off dock.	Taylor
		Section of the old dock with something on it that reflected light rode in on the wall of water. Wall of water visible before sheet pile cells disappeared.	K. Wallin
		Taylor looked over his shoulder as he started to run, saw D-7 Cat tilt.	Taylor
		Garoutte saw Taylor run by crane - he jumped out of the crane	Garoutte
		Cells actually drop out of sight - wall of water rushed in and enveloped area, saw D-7 Cat first tilt, hesitate, and then roll into water.	Garoutte

		P. Wallin disappeared as a huge wall of water and debris came crashing over him	K. Wallin
		Everything goes into the water	Young
		Garoutte started to run down the dock	Garoutte
7	6 Sec.	Blue work barge visible above bull rail	Taylor
8	10-14 Sec.	Garoutte overtook Taylor	Garoutte
9	15-16 Sec.	Ran about 200 feet down the dock	Taylor
		Ran slightly further than Taylor	Garoutte
10	16 Sec.	Taylor & Garoutte stop	Garoutte
11	17-19 Sec.	Garoutte saw ferry terminal lights disappear from view as wave or something blocks line of sight	Garoutte
		Taylor gets in pickup, looks at watch - 7:12 p.m.	Taylor
12	18 Sec.	Heard tremendous loud crash and boom from direction of ferry terminal. (Since Taylor did not hear this noise, Taylor was probably already in his pickup.)	Garoutte
13	24-34 Sec.	Garoutte ran back to crane	Garoutte
14	25+ Sec.	Taylor drove to City Hall	Taylor
15	60+ Sec.	Garoutte realized Paul Wallin was missing and ran back down the dock to call 911 at phone by boat harbor.	Garoutte
16	120+ Sec.	Garoutte returned to crane and started to search for Wallin. Saw a section of the old south dock with the gangway on it floating near the end of old north dock where Cells #4 and #5 had been	Garoutte
17	Later	Police arrive - search for Paul Wallin continued	Garoutte
18	Later	Karl Wallin told Bill Taylor that the deck section of the dock with the gangway on it they had seen coming in on the wall of water hit the end of the north dock where he was standing.	Taylor

From the approximate timing of events 6 and 7, a rough estimate of wave speed at the PARN site can be calculated in the 70-mph range. (Rational calculation using the formula $v = \sqrt{gh}$ gives a wave speed in the range of 50-60 mph) This being the case, the south end of the old PARN dock where the gangway was stored was destroyed at least 7 seconds prior to the wave arrival at the construction site.

Common sense dictates that since the wave destroyed the south end of the old dock first, and carried a section of the deck with a gangway on it essentially down the dock axis, the cause of wave could not be at the construction site.

It should be noted that Paul Wallin was standing on the inlet floor when he was inundated in a huge wall of water and debris. The tsunami carrying south dock debris arrived at the work site before the ground at the construction site slid in the inlet, which is conclusive evidence that the event did not start of the construction site.

Eyewitnesses Taylor and Garoutte reported the calm before the wave. It is estimated that the calm was between 1 and 2 minutes prior to the wave, based on the description by Taylor as to his actions.

The police report taken from Bill Armstrong (who was on a boat in the small boat harbor) confirmed that a wind gust arrived first and then the boat hit bottom. It can be concluded that the change in atmospheric conditions occurred first, followed by a drawdown of the waters in the small boat harbor.

The NOAA tide gage, which was situated near the Broadway Dock, recorded an initial drawdown followed by a crest wave.

A reexamination of the bathymetry of Taiya Inlet was next undertaken.

Evidence of a major underwater landslide, coincident with the extended axis of the south dock, was very apparent. It was located between 4,000 and 6,000 feet from the end of the south PARN dock.

The topography of the landslide scarp showed that its direction was southerly (down the inlet) and that a crest wave would be created down the inlet and trough wave (drawdown) would occur northerly toward Skagway. The crest wave would compress the air in its path, and an atmospheric pressure change would result. This air shockwave (similar to that which precedes a snow avalanche) would oppose the incoming southeast air movement (storm wind) and could create a period of calm. By the same token, the drawdown northerly of the landslide would create a pressure drop behind the slide area and replacement air would rush southerly from the north. This inflow was probably the wind "surge" felt by Armstrong before his boat hit bottom. This southerly flow could also cause an atmospheric change at the construction site.

About the time reevaluation of the entire body of facts and evidence commenced, PN&D took two very important additional steps to further define what occurred on November 3, 1994.

The first was to calibrate an identical tide gage to one installed at Skagway by the NOAA. PN&D owned an exact duplicate of that gage. As mentioned earlier, these tide gages are damped so as to record only long-period waves (tides) accurately. PN&D set up a laboratory test using a 30-foot salt water filled stand pipe to determine what actual wave configuration would duplicate the damped trace recorded on November 3, 1994, at Skagway on the NOAA gage.

PN&D also constructed a scale model (1/600) of Taiya Inlet at Skagway, filled it with water, and conducted a series of tests, which represented landslides at various locations within Taiya Inlet. The results of tests were videotaped so that slow motion viewing could occur, and simultaneous events that could not be adequately studied in real time viewing could be observed in slow motion.

The NOAA tide gage trace shown in Figure 3 provides a considerable amount of information but raised a question that PN&D 's testing attempted to answer.

The very first gage trace was a puzzle since times shown in Figure 3 as "X" and "Y" were both equal, which is an impossibility for long-period waves because the damped gage could not physically respond to both a crest and drawdown at nearly the same time.

Further testing was conducted to explain the initial "X" and "Y" traces recorded on the NOAA gage. It was determined that the tide gage pen responded instantly to a rapid atmospheric pressure decrease, a fact previously unknown. Such a rapid atmospheric pressure change caused by the initial wave as described above, undoubtedly caused the NOAA tide gage to "spike" just as its sister test gage did under similar circumstances during the PN&D test. It is true that these tide gages are pressure compensated but they require measurable time to react and compensate. Instant pressure changes do affect the gages.

The remainder of the trace recorded by the NOAA gage was readily duplicated during PN&D's testing. Combination of the stand pipe calibration trace and the atmospheric test data trace essentially duplicated the actual NOAA tide gage trace. The actual wave heights at the NOAA gage were now determined(7).

Tests in the 1:600 scale model constructed representing a Skagway Harbor area provided additional data. The model was filled with water and waves were created by rolling a cylindrical sand bag downslope in various directions to qualitatively represent slide movements.

A landslide originating at the construction site (dock slide) as theorized by some other investigators produced an initial crest wave at the gage and a following wave train that did not resemble the NOAA tide gage trace. Additionally, the State ferry dock moved eastward which was opposite to the direction it actually moved.

A landslide down the inlet (i.e. southerly) produced an initial drawdown at the gage and a following wave train similar to the NOAA tide gage trace. The State ferry dock moved to the west in concert with the physical evidence. The direction of the ferry terminal movement was consistent with Kowalik's analysis(5).

Wave heights could not be reliably measured in the model tests but the waves observed near the model construction site were significantly higher than at the NOAA tide gage location (Figure 1), again in concert with the physical evidence.

One of the most important pieces of physical evidence available to the investigation was the bathymetry of Taiya Inlet taken immediately after the event by PN&D. Much can be determined by the analysis of these data. The soundings were basically accomplished on November 7 through 9, 1994, and used state of the art GPS and a recording fathometer.

A first step in this portion of the reanalysis was to plot post-event contours of the sea floor utilizing the PN&D data (Figure 4) and pre-event data obtained from NOAA, PN&D, and others. While there was some pre-event data in the immediate PARN dock area, the remainder of the inlet was defined pre-event primarily by USC&GS (now NOAA) random soundings that, with some exceptions, were taken about 50 years ago. A comparison of these old data with newer data in the PARN dock area disclosed that the Skagway River had substantially increased its delta over this time span.

Transverse inlet cross-sections were plotted at 200-foot intervals. These cross-sections showed ridge and scour areas on the inlet floor. (Figure 5). Observations of these data disclosed that two major and one minor well-defined ridges existed longitudinally in the delta area. These long, narrow flat-topped ridges could not have been formed independently of the surrounding area. They were obviously remnants of the delta floor before the event occurred. By noting the high spots of the various flat-topped ridges on the cross-sections, it was possible to plot the longitudinal ridge profiles. These profiles were smooth and presented typical delta surface profiles, which became less steep as the distance from the river's mouth increased. Most importantly, the two major ridge profiles were nearly identical in slope and elevation, indicating that the flat ridge tops did indeed represent the original delta surface prior to the event.

Since these ridges defined the pre-event inlet floor, it was possible to connect the high spots on the flat-topped ridges and reconstruct the inlet floor prior to the event. This process allowed approximate reconstitution of the inlet floor elevation prior to the event within relatively close tolerances. (Figures 5 and 6)

When cast against the post event inlet floor elevations, these data supported a rational computation of the delta landslide volume. The following incremental volumes were determined. The four major slide areas are shown in Figures 4 and 6.

Slide 1	11[M]	cubic yards	delta landslide
Slide 2	5[M]	cubic yards	delta landslide
Slide 3A,B,D	3[M]	cubic yards	retrogressive slide
Slide 3C	3.6[M]	cubic yards	(retrogressive slide gully later filled by subaerial slides off the eastern slope of Taiya Inlet)
	22.6[M]	cubic yards	

[M] = million

These amounts represent net, not gross, slide volumes. It is quite probable that additional slide areas existed, but all or portions were filled in with secondary slides that occurred after the main event. There is no way that the volumes of such in filling of original slides can be determined at this time.

An interesting portion of the earth movement analysis was centered on the eastern slope of the inlet, between approximate Stations 6 and 34 (construction site southerly ½ mile), see Figure 4. The PN&D after-survey, coupled with the recent (1994) pre-event bathymetry in the PARN dock area, provided a very accurate portrayal of the before and after topography of the eastern Taiya Inlet side slope area. These data disclosed that side slope slides occurred along the entire slope in the area listed above. The slide that destroyed the sheet pile cells in the construction area at the PARN dock was at the very northerly end of these side slope failures. These slope slides have been coined as "subaerial slides" in order to give them a separate and distinct identification.

The side slope slides, as disclosed by the cross-sections, were "slices" of more or less uniform thickness at any specific location. This fact leads only to the conclusion that the cause of these side slope slides was undercutting of the slope toe, because no other slide mechanism will produce a "slice" type failure. The circular slope failure mechanism (gravity slide) does not produce a slice profile. A channel (gully) of some ilk had to have been present at the toe of these side slopes in order for the toe to be undercut. (Figure 7).

The incremental slide volumes decreased uniformly from south to north simply because the depth of toe undercutting also decreased uniformly. A decrease in gully depth is typical of a retrogressive slide gully that eventually daylights* headward on the original sea bottom. These side slope slides simply filled the gully that caused them to occur. The existence of these filled gullies was generally confirmed by seismic studies performed in November and December 1994, which disclosed "transparent soils" that had recently infilled the retrogressive gullies.

On the basis of this reanalysis, it was again concluded in the January 28, 1997, report(2) that the initial delta landslide occurred approximately 4,500 to 6,000 feet southwesterly from the end of the old PARN dock as shown by the bottom contours created from the PN&D November 1994 survey. Retrogressive gullies (slides 3A, B, C & D) were created as a result of the initial slide seismic

*Daylight is the point where the bottom of the gully intersects the original inlet floor.

vibrations. These were located easterly of the initial slides and shown in Figure 4. The most easterly retrogression had at least two arms with a small ridge between. It was the easterly arm of this retrogressive gully that undercut the easterly slope of Taiya Inlet and caused the side slope (subaerial) slides, the most northerly of which destroyed the southern portion of the PARN dock and the new sheet pile construction.

The slide that destroyed the sheet pile cells at the construction site was the very last to occur—not the first, and was not caused by activity at the PARN construction site. This reanalysis only confirmed the original 1995 analysis.

Confirmation Phase

After the January 28, 1997, in-depth reanalysis of the Skagway River delta landslide was issued, still more investigators made additional studies. Four additional studies not only confirmed initial factual findings but also shed new light on some details of the event:

1) Charles Mader performed a mathematical analogy of tsunamis created by various slide scenarios at different locations in Taiya Inlet(6).

2) A submersible vehicle was used to perform an underwater inspection of a portion of Taiya Inlet(8).

3) A further interview with eyewitness Stan Selmer added new information(3).

4) NOAA performed a detailed underwater bathymetry survey of nearly the entire Taiya Inlet(4).

Mader provided the first confirmation by analyzing several possible slide scenarios using a computerized mathematical analogy known as SWAN developed at Los Alamos as a basis for predicting flood levels in coastal areas of the United States that might result from asteroid impacts in the Atlantic and Pacific Oceans.

Of specific interest were two possible slide locations. The first was the 4-million-cubic-yard± slide off the eastern shore of Taiya Inlet, which Mader coined the "dock landslide," and identified as "subaerial slides" in the 1995 and 1997 analyses. This slide was theorized by other investigators to be the cause of the tsunami. The second location was the 22-million-cubic-yard± Skagway River delta landslide that occurred roughly one mile southwesterly of the PARN dock.

As a result of his 1997 study, Mader concluded that the "dock landslide" could not have been the cause of the tsunami for several reasons.

It produced a tsunami with a period of only approximately 1 minute, while the NOAA tide gage revealed an actual tsunami period of 3 minutes. The amplitude of the "dock landslide" tsunami wave at the tide gage was only about half of that actually recorded on the tide gage and described by witnesses. Its direction was approximately 90° different than the direction observed by eyewitnesses.

Further, the "dock landslide" produced an initial crest wave at the tide gage instead of an initial drawdown as actually recorded. The 4-million cubic yard dock landslide sustained a seiche in Taiya Inlet of only about 6 minutes, while the tide gage recorded a 30-minute-plus seiche.

In contrast, Mader found that the 22-million-cubic-yard±-delta landslide produced a tsunami with a 3-minute period similar to that recorded on the tide gage. This tsunami had a wave amplitude similar to that recorded on the tide gage and observed by eyewitnesses as well as sustaining a seich of over 30-minutes as actually recorded. In addition, the tsunami direction was similar to the direction observed by the eyewitnesses and caused a drawdown to initially occur in the upper Taiya Inlet as actually recorded on the NOAA gage.

Mader's findings indicated that the 22-million-cubic-yard delta slide was the cause of the tsunami, not the 4-million-cubic-yard dock slide.

A second confirmation occurred when Plafker & Greene(8) conducted an underwater viewing of Taiya Inlet utilizing a two-man submersible craft. Unfortunately the persons doing the underwater observation were not made aware of the plethora of information that was already available when the underwater excursion was conducted in June 1998(4).

Without this important preexisting data, their efforts were focused on the subaerial "slice" slides that occurred along the easterly slopes of Taiya Inlet (Mader's "dock slide"), and not on the major landslide that occurred in Taiya Inlet.

Their underwater observations led to several conclusions.

The subaerial slides along the eastern slope of Taiya Inlet were of slice undercut configuration as opposed to a circular slip slide. (This visual configuration determination is also consistent with the "before" and "after" bathymetry data obtained in 1994 by PN&D.)

The slide materials filled the retrogressive gully that created the undercut of the toe of the slope. These slides progressed from south to north. The slide at the construction site was hence the last to occur—not the first as had been theorized by other investigators.

The underwater observations also confirmed that the subaerial slides occurred in basically two steps as reported in the January 28, 1997, analysis. The initial "slow portion" of the slides occurred as the retrogressive channel undercut the toe of the slope. The "fast portion" occurred as the tsunami wave changed the inlet water level at a particular slide site from perhaps –35'± MLLW to 25'± MLLW in a manner of about 1.5 minutes.

As part of the overall investigation by Plafker and Greene, an on-the-ground search of the tidal area in Taiya Inlet was conducted. This search disclosed evidence that the tsunami reached an elevation of roughly +30' MLLW at Stargills Creek (on the east side of Taiya about 2 miles southerly of the PARN dock). This elevation is about 6 to 8 feet above storm-driven high tide. At Burro Creek, on the west side of Taiya Inlet across from the PARN dock, no evidence of a tsunami wave in excess of a normal high tide was found. Comparison of these observations with Mader's mathematical analysis show that such events are consistent with a tsunami created by the 22-million-cubic-yard±-inlet delta slide, but are totally inconsistent with the tsunami created by a 4-million-cubic-yard± subaerial slide.

Another confirmation was achieved during an interview with Stan Selmer (Mayor of Skagway) in June 1997. He stated that when he arrived at the small boat harbor (just after the second crest wave occurred on November 3, 1994), the harbor entrance was plugged solid with debris and it was impossible for a rescue boat to exit the harbor. The debris was from the south dock, which had been completely destroyed.

The fact that all the debris was piled against the boat harbor breakwater and plugged the exit at the first crest of the seiche disclosed that the tsunami direction was from the south dock toward the harbor breakwater (southwest to northeast). Such a wave direction could not occur if the source of the tsunami had been caused by the subaerial slides off the eastern limit of Taiya Inlet, as the debris would have been out in Taiya Inlet, not in the small boat harbor.

The last, and perhaps most convincing, confirmation occurred in May of 1998 when NOAA sent its underwater sounding equipment to Taiya Inlet aboard its ship Rainier and performed a very detailed, precise interrogation of the sea floor in Taiya Inlet. This bottom survey extended over essentially the entire area of Taiya Inlet and allowed the production of exquisitely detailed mapping of the inlet floor. This NOAA investigation confirmed the accuracy of the PN&D November 1994 bottom survey.

As part of the NOAA investigation, it displayed its data on a color-based, shadowed projection, which gave a colored, 3-D pictorial view of the inlet. A review of the projections instantly discloses the location of the major delta landslide and the resultant retrogressive gullies. Since the subaerial slides were caused by a toe undercutting retrogressive gully, which in turn was filled by the slide, there is little physical evidence of that occurrence detectable on these NOAA 3-D projections. A similar non-colored before and after pictorial is shown in Figure 6. The NOAA colored 3-D pictorial views are shown in Figure 8.

The huge underwater landslide scarp shows in detail, and is almost a textbook example with regard to configuration. It is abrupt and crescent-shaped as is typical of this natural occurrence. The two major retrogressive slides, which resulted from soil liquefication amplified by the delta slide seismic vibrations, again represent excellent textbook examples of such occurrences. Both diminish in depth as they progress headward until they daylight on the inlet floor.

Conclusions

When one looks at all the evidence and facts concerning this event, only a single conclusion can be reached that satisfies all the evidence. The Skagway River delta landslide in Taiya Inlet, about 4,500 to 6,000 feet southwest of the old south dock was the cause of the tsunami that occurred at Skagway at about 7:10 p.m. on November 3, 1994.

The underwater delta of the Skagway River suffered a major collapse at a very low tide soon after a major flooding had deposited a large amount of material on the upper delta. This initial collapse (landslide) contained at least 11 million cubic yards.

An ensuing ocean level drawdown and ground shaking (vibration) similar to a miniature earthquake resulted from the large landslide and caused liquefaction of other portions of the Skagway River delta and retrogressive gullies occurred that daylighted near the northern end of Taiya Inlet.

One arm of one of these retrogressive gullies undercut the eastern slope of Taiya Inlet and slice slides occurred off the slope and filled the gully. The incremental size of the slides was controlled by the depth of the gully at a particular increment location. Since the gully lessened in depth as it eroded headward, the incremental slides decreased in volume. The last increment to occur was at the construction site. Since this last incremental slide at the PARN construction site occurred long after the inlet delta slide, it was neither the cause nor trigger of the delta slide and subsequent tsunami.

A large tsunami followed the collapse and rose to an elevation of about +30' MLLW (35' amplitude) southerly of the landslide area near Stargills Creek. Concurrently a drawdown occurred northerly of the landslide and was followed by a crest that reached approximately 25' MLLW elevation (30' amplitude) at the PARN construction site. This was the tsunami that caused much of the damage to the man-made objects in the upper inlet.

Theories purported by other investigators that the tsunami was caused by a slide created by construction activity at the PARN dock are totally inconsistent with the evidence and hence cannot be correct.

A review of existing literature concerning similar events (especially in Norway) discloses that probably no other event has been so completely analyzed and totally dissected as the Skagway November 3, 1994, delta collapse and resultant tsunami.

Future Action

Tsunamis at Skagway are of a local nature caused by submarine landslides. Slide triggering mechanisms can be from either seismic activity or very low tides usually following Skagway River flooding.

Some predictable things are known at Skagway. The Skagway River provides sediment to slide areas; thus river flooding is a sign of sediment buildup and a warning of forthcoming tsunami potential. Non-seismic tsunami activity usually occurs during very low tides following periods of river flooding. With all these things in mind a tsunami warning system at Skagway probably should include both measurements and education.

Instrumentation in the form of a recording stream gage could produce results directly related to river sediment transport and underwater sediment buildup on the delta. Periodic bathymetric comparative surveys of critical delta areas would verify stream gage predictions concerning sediment buildup.

A tsunami in Taiya Inlet caused by an underwater Skagway River delta landslide could present a hazard to Skagway especially with the several thousand tourists a day that visit from large tourships during summer months.

In the past, these events have occurred at very low tides. Since Skagway has a tidal range of about 27 feet, any Tsunami would have to have a crest in the range of 25 to 30 feet in order to exceed the high tide line if it occurred at low tide. A tsunami of this size could be expected to have a period in the range of 3 minutes.

Since a drawdown would occur first in the Skagway harbor area, only about 1.5 minutes are available for warning after a drawdown is observed until the following crest wave occurs.

A continuous digital reading tide gage could detect unusual occurrences in Taiya Inlet and perhaps serve as a basis of alarm. Offshore seabed monitors located at suspected slide areas and connected to sirens and/or lights might also increase warning time.

Boat owners and coastal users need to be informed about conditions that could produce a tsunami. They also need to know the significance of various parts of the tsunami warning system. The "Cry Wolf" syndrome must be carefully avoided with observation and coastal evacuation plans firmly implanted and emphasized.

Given the large tourist population in Skagway during the summer, it might be prudent to inform the tourship operators of predictable very low tide events and encourage ship-berthing schedules away from those times.

The principle culprit in the entire tsunami problem is the Skagway River in its diverted location. Historically the river formed its river delta by meandering and distributing sediment uniformly over the delta face. As civilization advanced to the waterfront, the river has been diverted to one very restricted location, thus river borne sediment deposits became concentrated and very large sub-sea slides, such as occurred on November 3, 1994, became a reality.

The obvious danger of a similar event occurring again in the future should be recognized and appropriate safety measures installed by responsible government officials. To do otherwise could constitute negligence now that the intricate anatomy of these destructive natural events is known.

References

1) Campbell, B.A., "Report of a Seafloor Instability at Skagway, Alaska, November 3, 1994," January 16, 1995.

2) Campbell, B.A., "Analysis of the November 3, 1994, Skagway Seafloor Instability," January 28, 1997.

3) Campbell, B.A., "Addendum to the Analysis of the November 3, 1994, Skagway Seafloor Instability," July 24, 1998.

4) Campbell, B.A., "Second Addendum to the Analysis of the November 3, 1994, Skagway Seafloor Instability," November 10, 1998.

5) Kowalik, Zygmunt, "Landslide-Generated Tsunami in Skagway, Alaska," Science of Tsunami Hazards, Vol. 15, No. 2, pp. 89-106, 1997.

6) Mader, Charles, "Modeling the 1994 Skagway Tsunami," Science of Tsunami Hazards, Vol. 15, No. 1, pp. 41-48, 1997.

7) Nottingham, Dennis, "The 1994 Skagway Tsunami Tide Gage Record," Science of Tsunami Hazards, Vol. 15, No. 2, pp. 81-88, 1997.

8) Plafker, George and Greene, Gary, H., "Report on the November 3, 1994 Submarine Landslide and Associated Landslide-Generated Wave at Skagway, Alaska," pp. 1-13, 1998.

9) Yehle, Lynn, A. and Lemke, Richard, W., "Reconnaissance Engineering Geology of Skagway Area, Alaska; with Emphasis on Evaluation of Earthquake and Other Induced Hazards," United States Geological Survey, 1972.

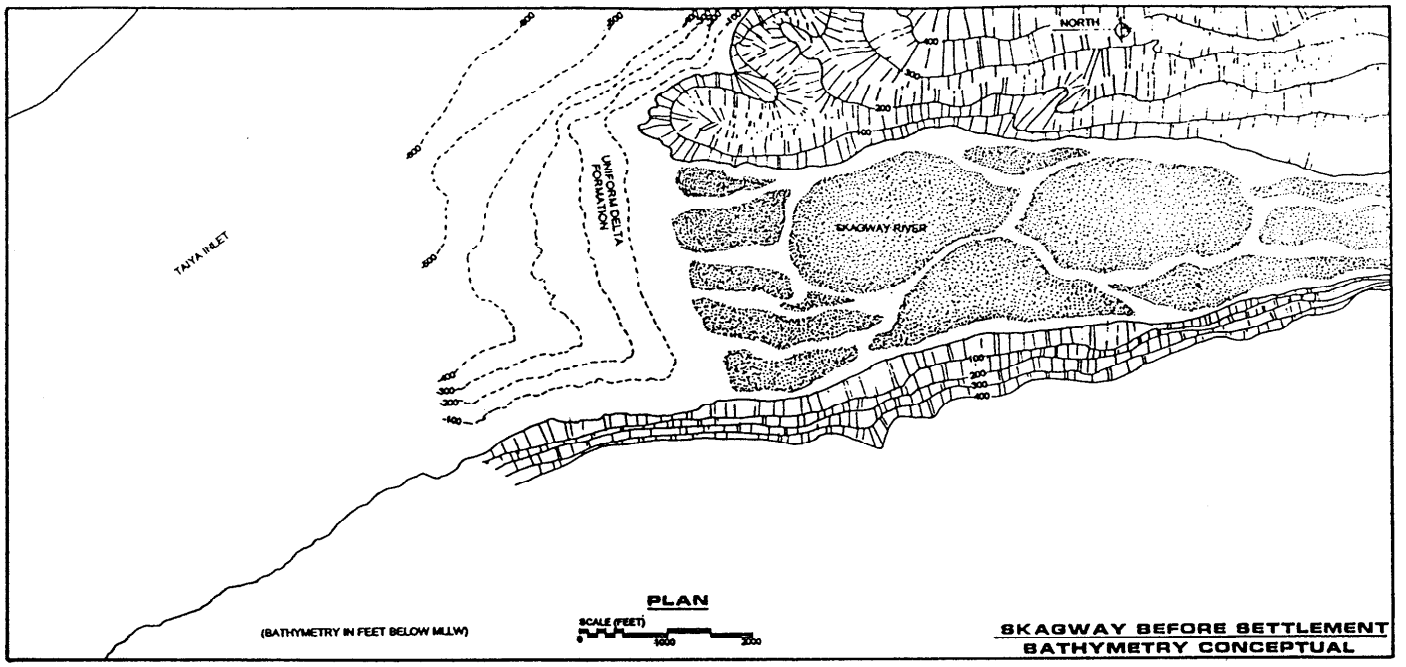

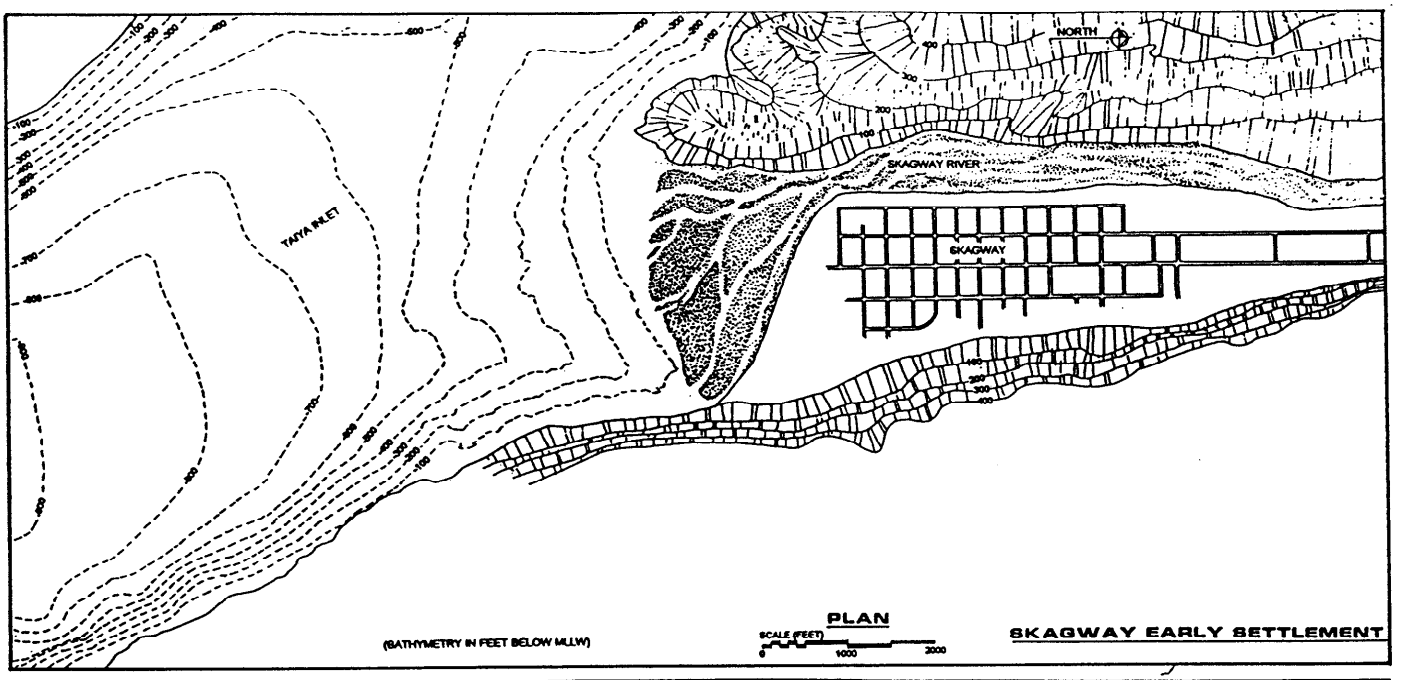

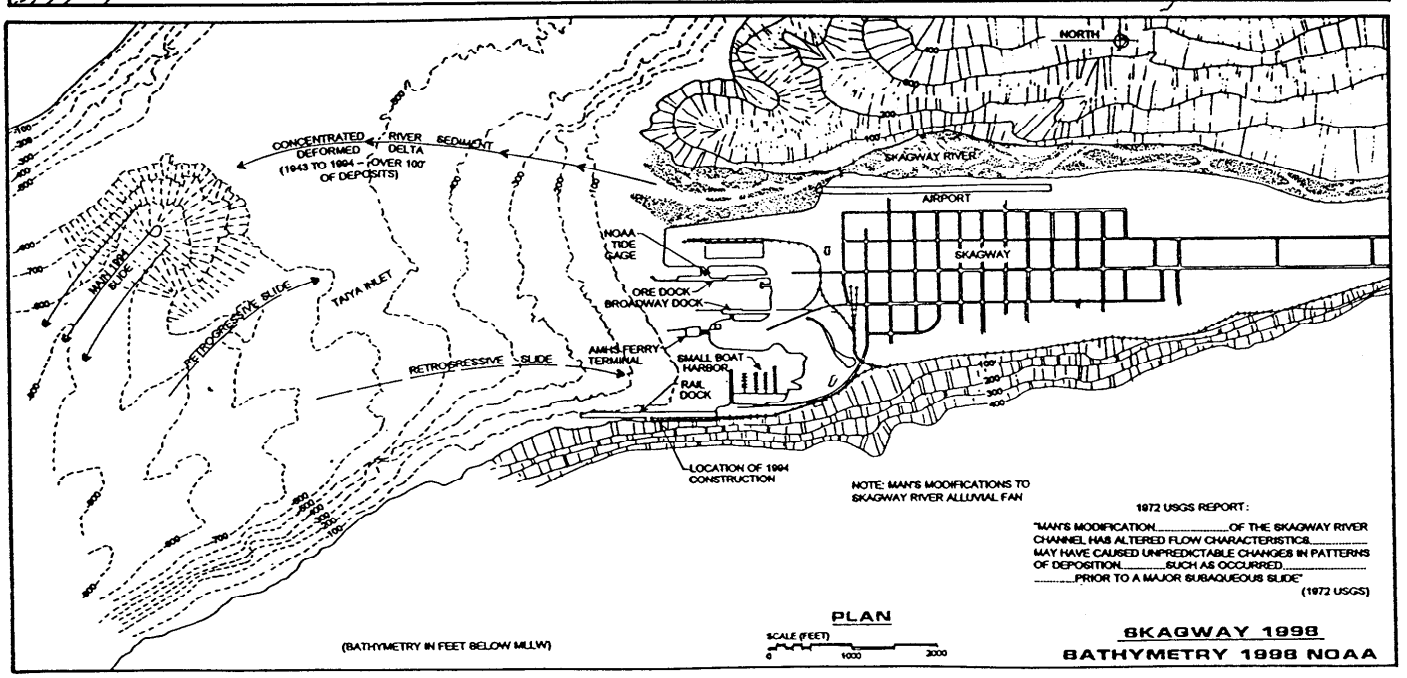

Figure 1 - Skagway Maps

Figure 1 - Skagway Maps

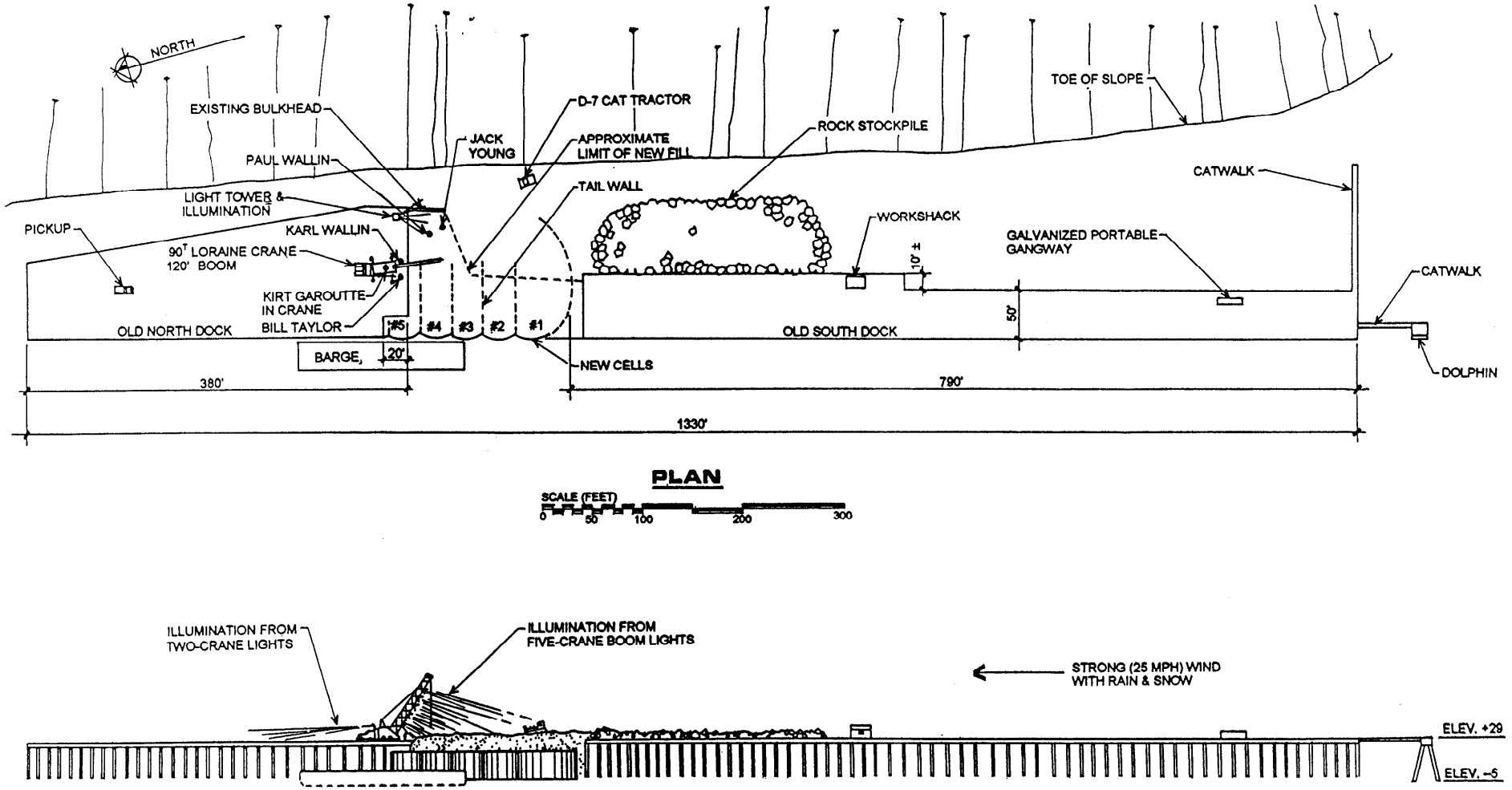

CONDITIONS BEFORE EVENT
Figure 2

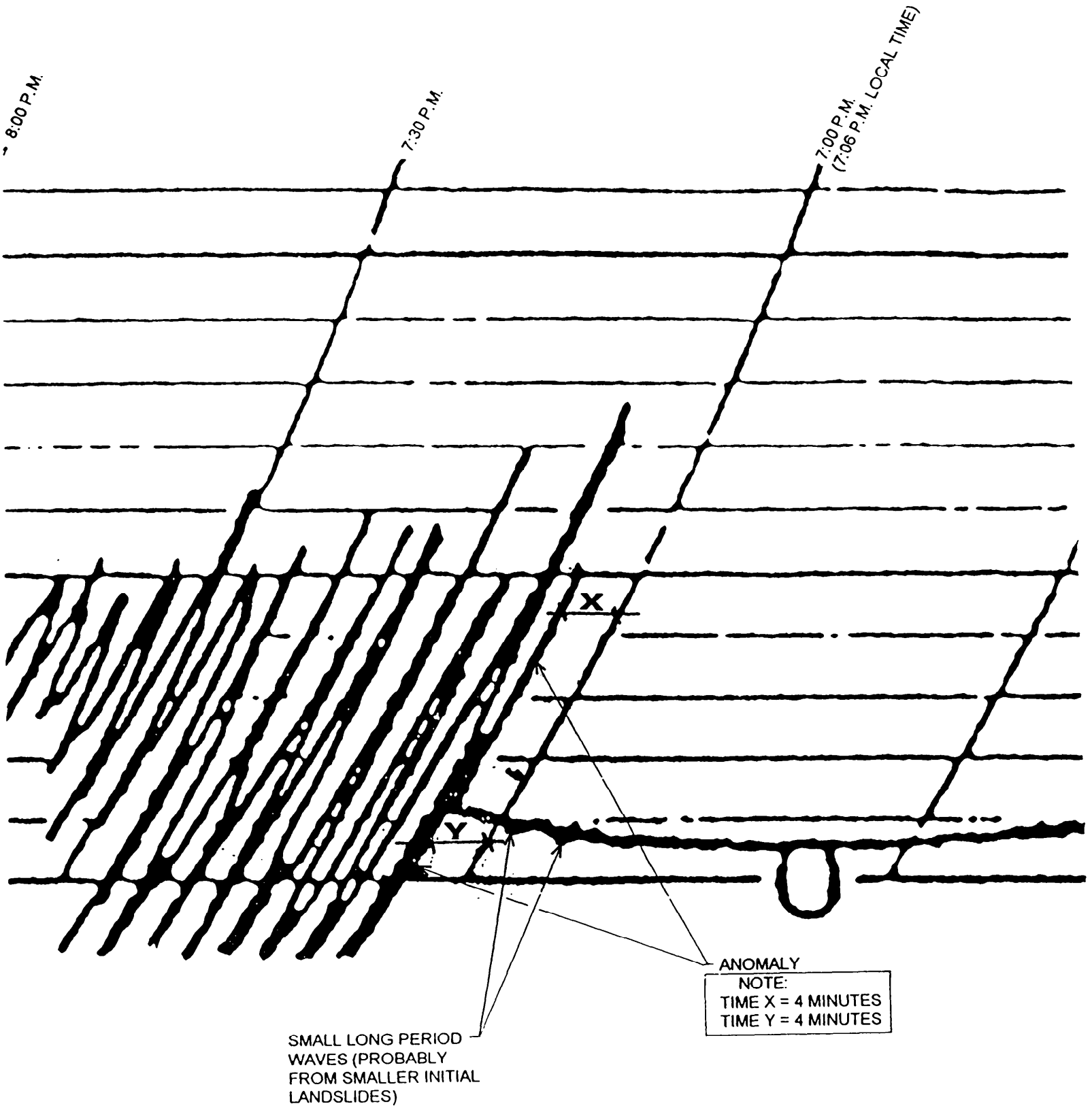

NOAA TIDE GAGE TRACE
Skagway, Alaska
November 3, 1994

Figure 3

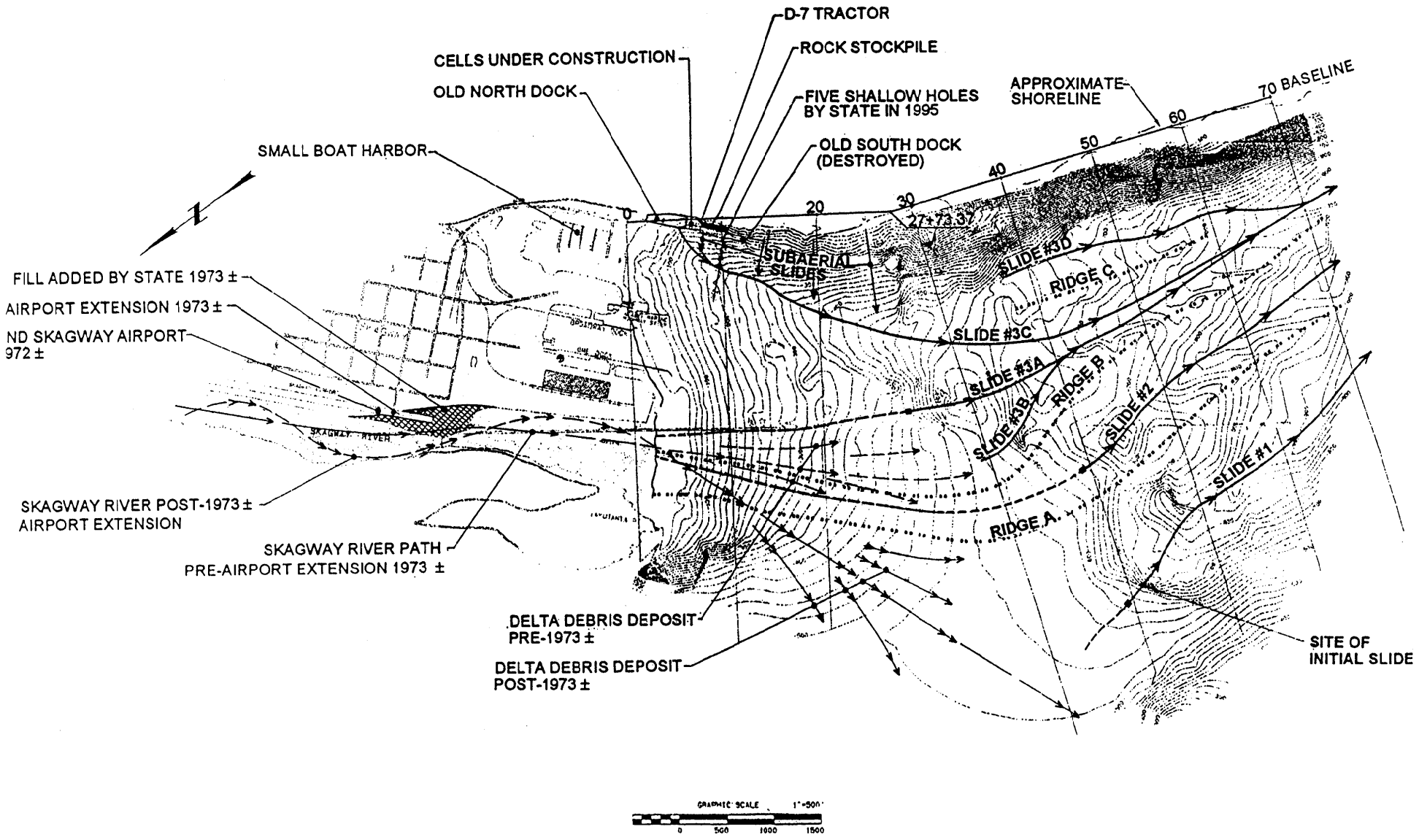

DATA SOURCE:
PN&D SURVEY 11/7-9/ 1994

POST EVENT SEAFLOOR CONTOURS
SKAGWAY, ALASKA
Figure 4

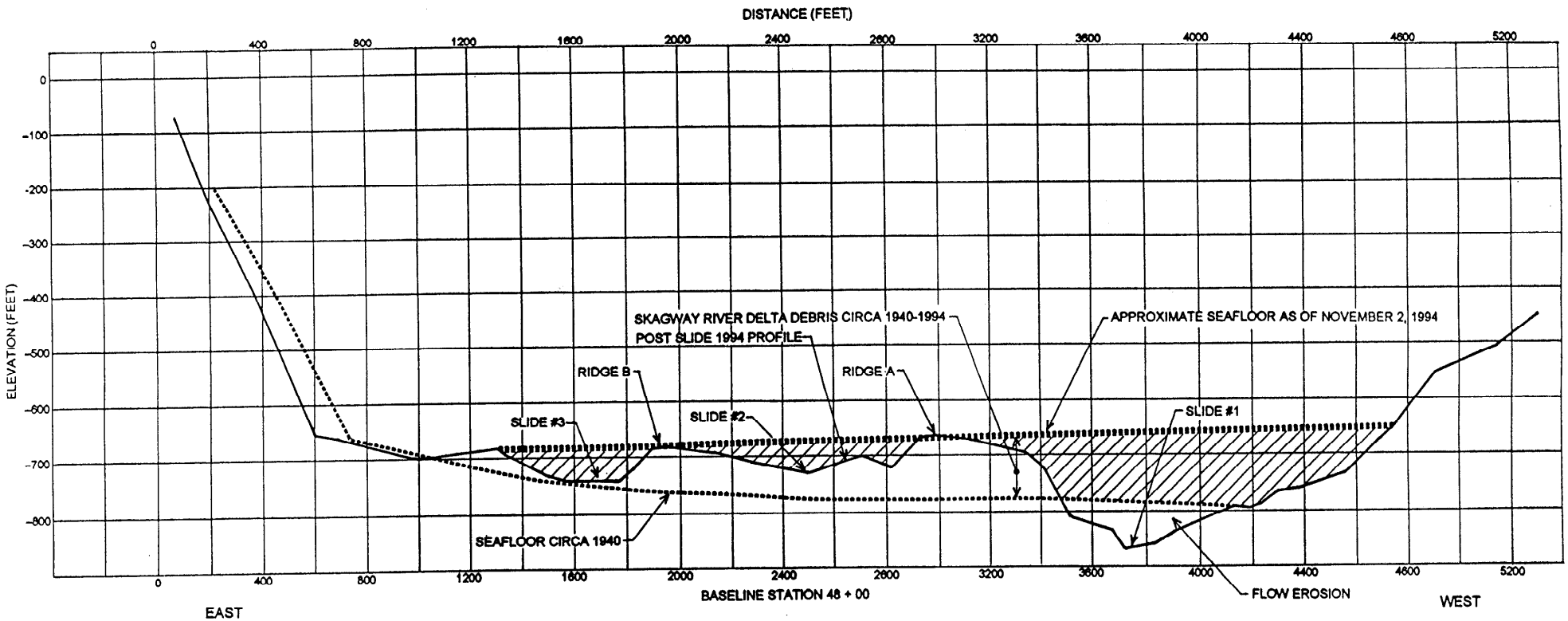

SECTION

TYPICAL TAIYA INLET CROSS SECTION
Figure 5

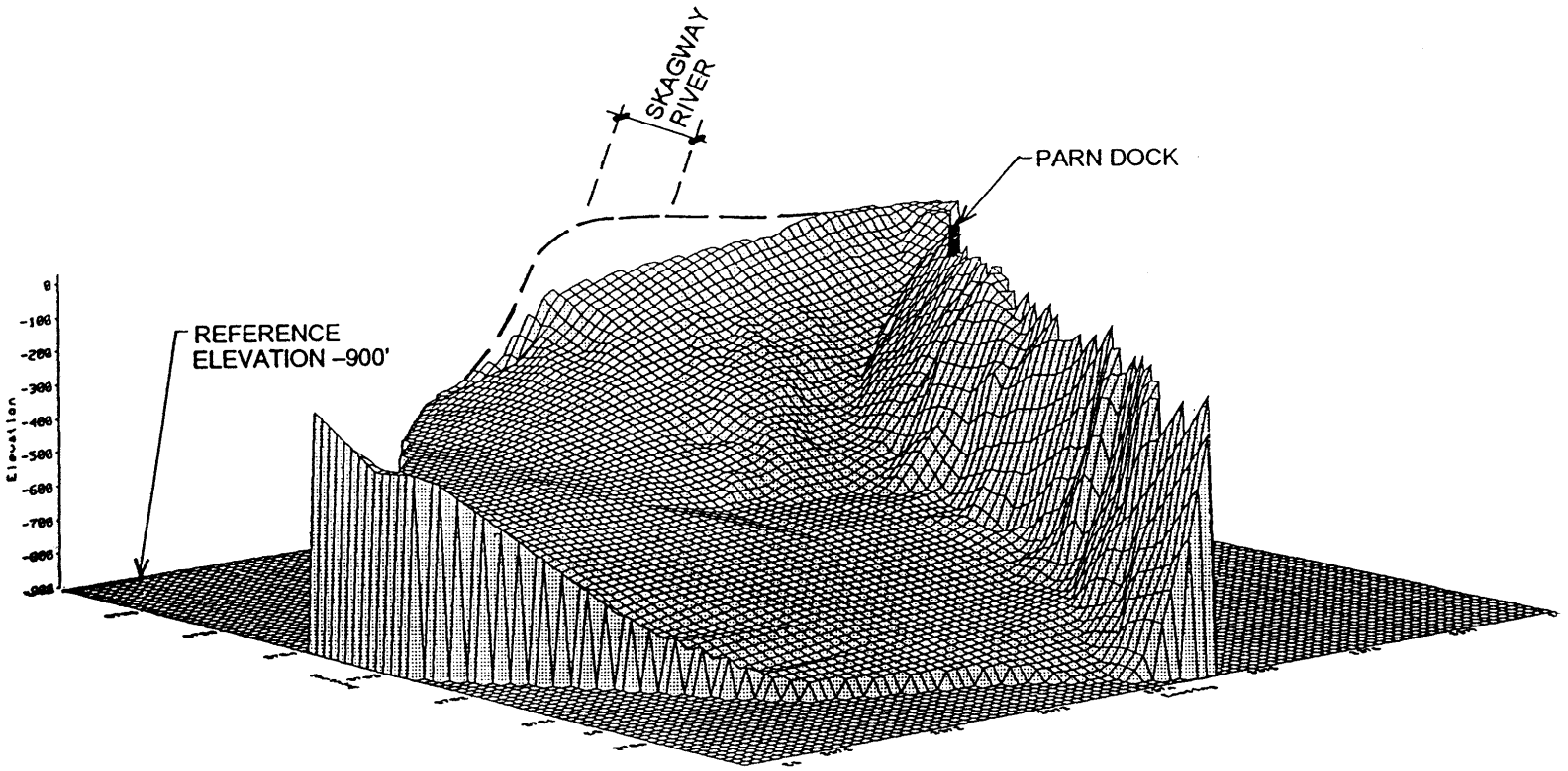

TAIYA INLET SEAFLOOR PRE-INSTABILITY

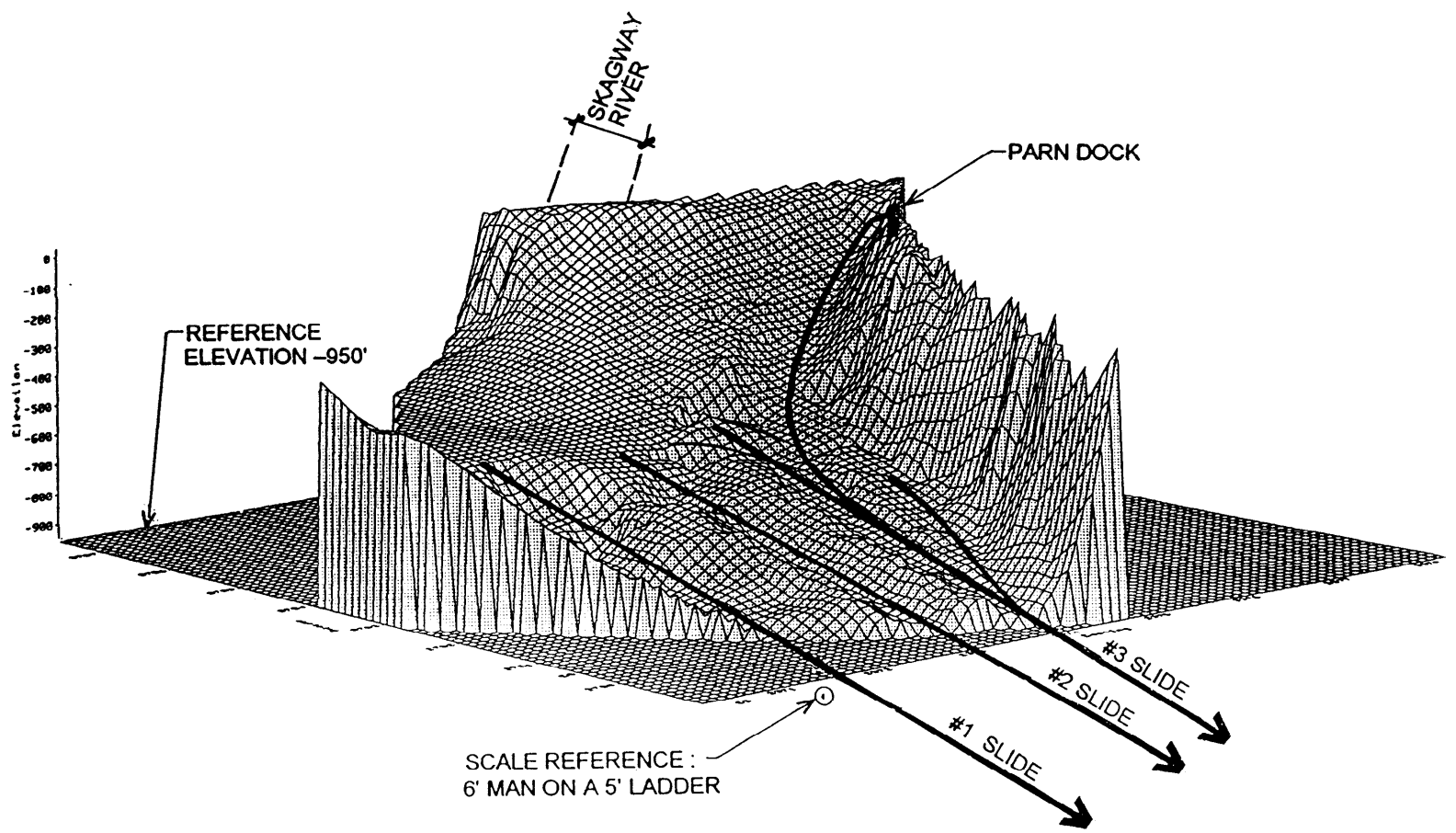

TAIYA INLET SEAFLOOR POST-INSTABILITY

LANDSLIDE 3D VIEWS BEFORE & AFTER
Figure 6

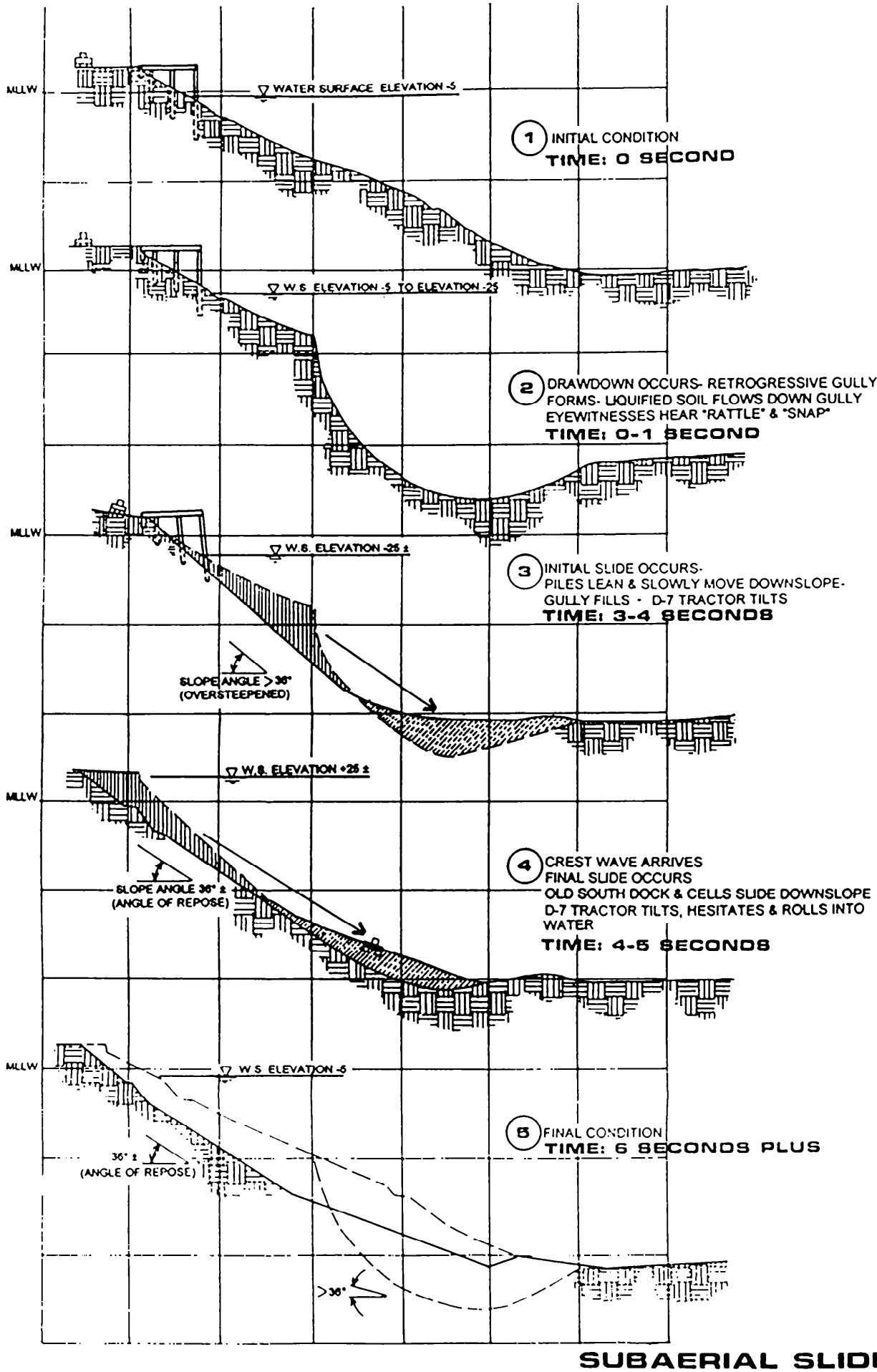

SUBAERIAL SLIDES
EAST SIDE OF TAIYA INLET
NOVEMBER 3, 1994

Figure 7

U.S. National Oceanic and Atmospheric Administration (NOAA)

Mapping

Shortly after the November 3, 1994, submarine slide and resultant tsunami, PN&D contacted the National Oceanic and Atmospheric Administration (NOAA) and requested them to map the underwater areas of Taiya Inlet with special focus on the area where the massive underwater landslide occurred.

NOAA responded in a positive manner, as they also were interested in the cause of the tsunami.

NOAA's first effort in 1995 mapped shallow water areas near the harbor that did not include the slide area. In 1998 they mapped nearly all of Taiya Inlet and produced astonishing maps, in color, that graphically show the recent areas of instability.

The enormity of the subsea slides is clearly visible to even the untrained eye in the NOAA 3D portrayals. Some notes have been added to NOAA graphics to point out important features.

NOAA preformed a very valuable public service in performing the extensive underwater mapping that accurately located the landslide that caused the tsunami that resulted in a fatality and damaged several waterfront developments in Skagway.

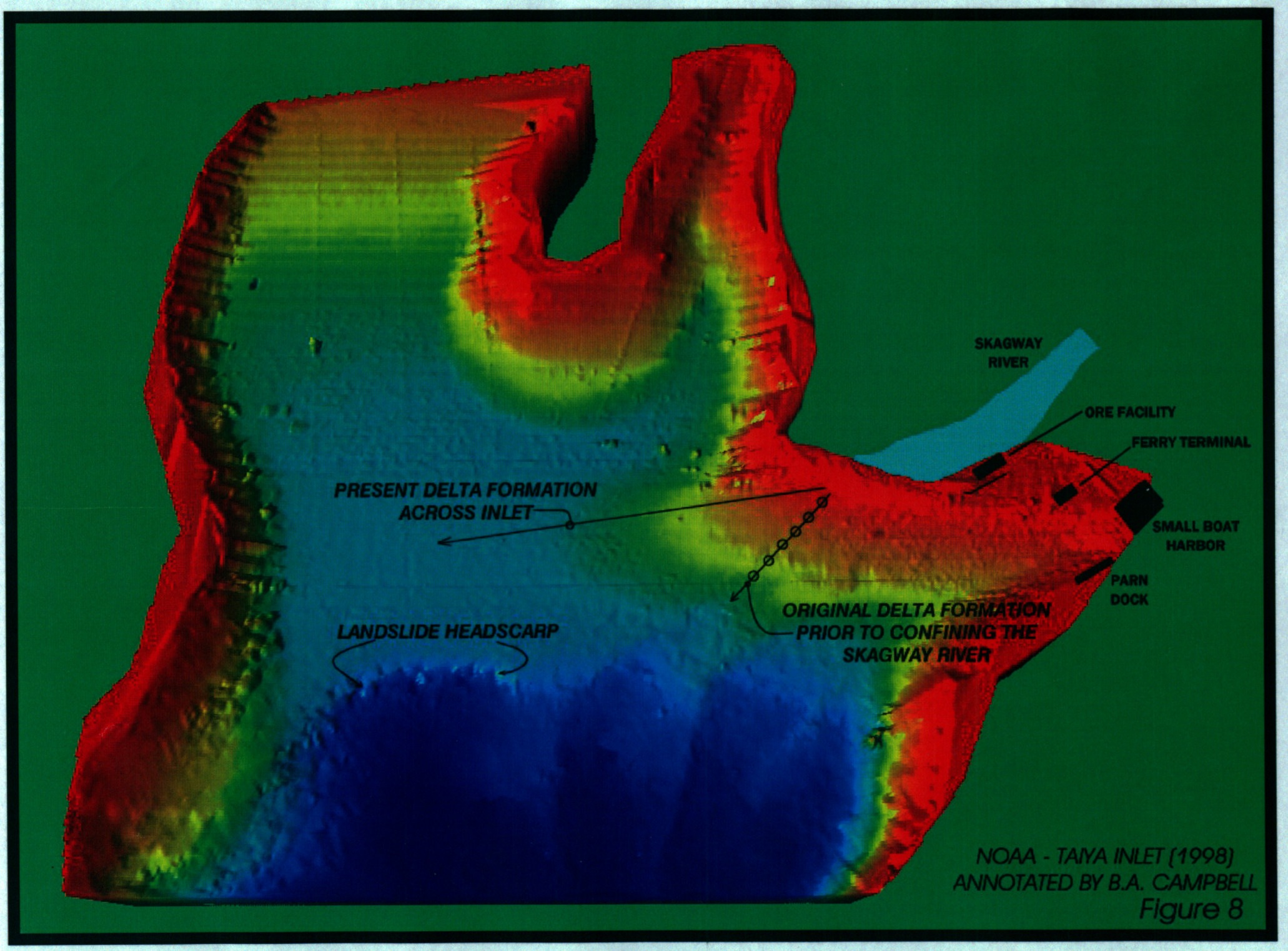
SKAGWAY
RIVER
ORE FACILITY
FERRY TERMINAL
PRESENT DELTA FORMATION
ACROSS INLET
SMALL BOAT
HARBOR
PARN
DOCK
ORIGINAL DELTA FORMATION
PRIOR TO CONFINING THE
SKAGWAY RIVER
LANDSLIDE HEADSCARP
NOAA - TAIYA INLET (1998)
ANNOTATED BY B.A. CAMPBELL

Figure 8

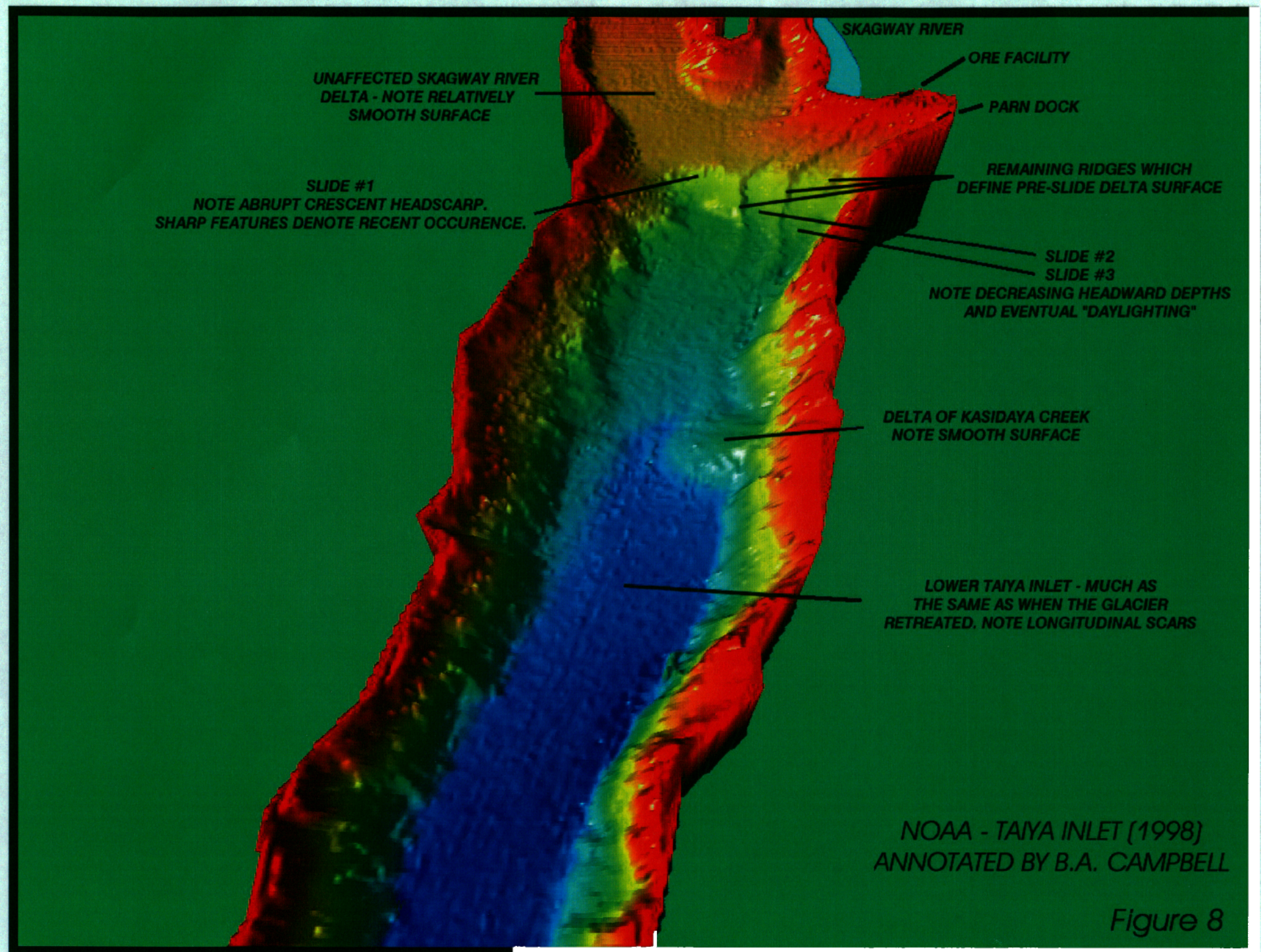
SKAGWAY RIVER
ORE FACILITY
UNAFFECTED SKAGWAY RIVER DELTA - NOTE RELATIVELY SMOOTH SURFACE
PARN DOCK
REMAINING RIDGES WHICH DEFINE PRE-SLIDE DELTA SURFACE
SLIDE #1
NOTE ABRUPT CRESCENT HEADSCARP.
SHARP FEATURES DENOTE RECENT OCCURENCE.
SLIDE #2
SLIDE #3
NOTE DECREASING HEADWARD DEPTHS AND EVENTUAL "DAYLIGHTING"
DELTA OF KASIDAYA CREEK
NOTE SMOOTH SURFACE
LOWER TAIYA INLET - MUCH AS THE SAME AS WHEN THE GLACIER RETREATED. NOTE LONGITUDINAL SCARS
NOAA - TAIYA INLET (1998)
ANNOTATED BY B.A. CAMPBELL

Figure 8

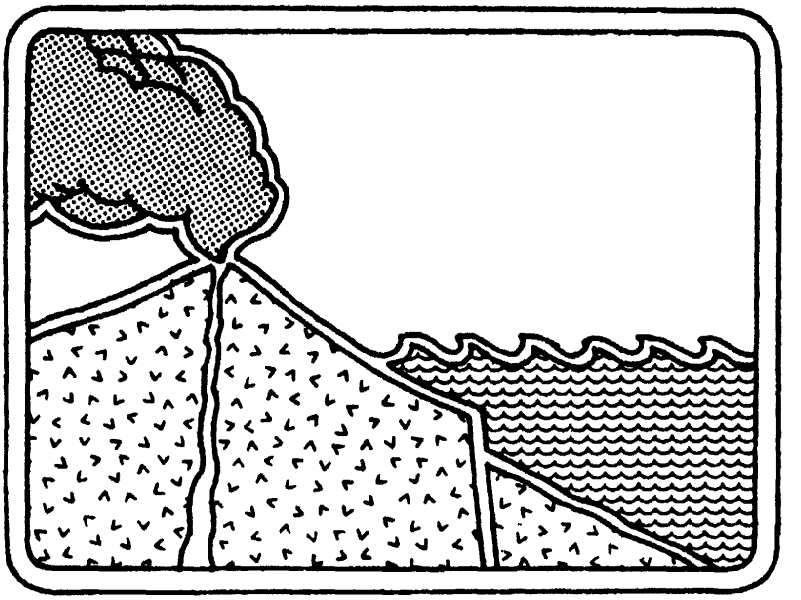

THE U.S. WEST COAST AND ALASKA TSUNAMI WARNING CENTER

Thomas J. Sokolowski
West Coast and Alaska Tsunami Warning Center
Palmer, AK 99645 U.S.A.

ABSTRACT

The Alaska Tsunami Warning Center (ATWC) was established in Palmer, Alaska in 1967 as a direct result of the great Alaskan earthquake that occurred in Prince William Sound on March 27, 1964. In 1996, the responsibility was expanded to include all Pacific-wise tsunamigenic sources which could affect California, Oregon, Washington, British Columbia and Alaska coasts and the center became the West Coast/Alaska Tsunami Warning Center (WC/ATWC).

An on-going project at WC/ATWC is the prediction of tsunami amplitudes outside the tsunami generating area described in *Science of Tsunami Hazards* **14**, *147-166 (1996).* The basic idea behind this technique is that pre-computed tsunami models can be scaled by recorded tsunami amplitudes during an earthquake to give a reasonable amplitude estimate outside the source zone. Tsunami models for moment magnitude 7.5, 8.2, 9.0 earthquakes have been computed along the Pacific plate boundary from Honshu, Japan to the Cascadia subduction zone. The modeling technique was verified by comparison to historic tsunamis from different regions. At present, the results from the scaled models are not distributed to the emergency officials during warnings, but are used only internally as an aid in canceling or extending warnings.

Another current project at WC/ATWC is to receive tsunami data from the Pacific-wide tsunami sites via a satellite phone system. Due to the current delay of 1 to 3 hours in receiving tide data from NOS gauges, selected windows of data can be received from these tide sites using a satellite phone, antenna, PC computer and special hardware inserted into the current NOS field packages. This will permit obtaining data from selected tide sites nearest the tsunami source.

WC/ATWC conducts a community preparedness program which provides advice and training sesssions to coastal citizens and emergency managers to aid in pre-event planning. The aim of the program is to educate the public to help themselves if they are caught in the middle of a violent earthquake and/or tsunami, and to be aware of the safety procedures, safe areas, and the limitation of the Tsunami Warning System.

The U.S.West Coast/Alaska Tsunami Warning Center(WC/ATWC) was established in Palmer, Alaska in 1967 as a direct result of the great Alaskan earthquake that occurred in Prince William Sound on March 27, 1964. This earthquake alerted State and Federal officials to the need for a facility to provide timely and effective tsunami warnings and information for the coastal areas of Alaska. In 1982, the WC/ATWC's area of responsibility(AOR) was enlarged to include the issuing of tsunami warnings to California, Oregon, Washington, and British Columbia, for potential tsunamigenic earthquakes occurring in their coastal areas. In 1996, the responsibility was again expanded to include all Pacific-wide tsunamigenic sources which could affect the California, Oregon, Washington, British Columbia and Alaska.

The Staff at the WC/ATWC consists of four geophysicists and 2 electronics technicians. The center is manned during normal week-day work hours. After normal work hours and on weekends and holidays, two duty personnel are on paid standby duty and must respond to the center within five minutes of an alarm. Alarms are activated by two different methods. The first is triggering by sustained amplitudes at 8 seismometers throughout the WC/ATWC's AOR. Alarms are also activated by a real-time seismic processing system when an earthquake exceeds a predetermined magnitude threshold for various regions throughout the Pacific basin.

To issue immediate tsunami warnings at any time during the day or night, it is vital that all electronic equipment, systems, and computers function as expected. The WC/ATWC's electronic staff is responsible for maintaining, monitoring, integrating, and enhancing complex electronic equipment at the remote sites and at the center. The WC/ATWC operates and maintains fourteen remote sites in Alaska. Each of these remote systems contains subsystems and other electronic components that are monitored frequently to ensure continuous transmission of quality data. These sites are visited once a year, and as soon as possible after equipment malfunction. At the WC/ATWC's operations center, there are numerous pieces of electronic equipment, such as, communication systems; satellite dishes; micro computer systems; un-interruptible backup power systems; recording and archiving systems; alarm systems; seismometers; data acquisition systems; calibrators; data telemetry radios; and numerous display monitors.

The WC/ATWC operates a real-time data network of twenty short and long period seismometers in Alaska, plus a local digital broadband station. Three more broadband seismometers are expected to be installed in 1999. As a result of the NOAA Tsunami Hazard Mitigation effort, the flow of real-time seismic data to the WC/ATWC has been significantly increased with the implementation of the Earthworm system (Johnson *et al.*, 1995). This front-end system provides the WC/ATWC the ability to receive/transmit digital seismic data with others who have an Earthworm system. Integrating this front-end with the WC/ATWC processing system permits over 80 channels of vertical short-period and long-period seismic data, and broadband seismic data to be recorded and processed at the

WC/ATWC. The WC/ATWC exchanges real-time seismic data with the National Earthquake Information Center (NEIC), University of Alaska, Alaska Volcano Observatory, Pacific Tsunami Warning Center, USGS Menlo Park observatory, University of Washington, Incorporated Research Institutions for Seismology, and Canada. Data from these other networks are available to the center in real-time over dedicated circuits.

The real-time seismic processing system at the WC/ATWC was developed and enhanced over the last 18 years (Sokolowski *et al.*, 1983; Zitek *et al.*, 1990). Real-time analog data and real-time digital data are immediately processed by a P-picking algorithm (Veith, 1978) which determines the onset of a P wave from an earthquake's signature. This algorithm works well on short period or filtered broadband data for both local and teleseismic earthquakes. An algorithm uses the P-picks to determine parameters for local, regional and teleseismic earthquakes. As more data are received and processed, automatic solutions continue until a predetermined amount of time has passed with no additional P-picks. The automatically determined earthquake parameters are immediately sent to duty personnel over the radio alarm system. The initial magnitude estimate is based on an Mb, Ml, or Mwp (Tsuboi *et al.*, 1995) depending on the size and location of the earthquake. Surface wave magnitude processing is triggered by the automatic locations. Ms magnitudes are automatically computed cycle-by-cycle as Rayleigh waves arrive at the long period and broadband stations.

The present seismic processing system uses Pentium PCs with the Windows NT operating system. Two identical PC systems are active for redundancy, plus for the added ability to process multiple aftershocks that are common with tsunamigenic earthquakes. A third system, another backup, is also operational to interactively locate an earthquake's parameters and to generate critical messages. It is purposely not integrated with any of the automatic processes. The automatic seismic processing PCs use a four-monitor card which displays information on four separate monitors. The displays on these monitors permit a geophysicist to view the real-time data, automatic P-picks, continuous long and short period waveform data, and an earthquake's data and solution parameters. This also permits a geophysicist to rapidly change P-picks and to re-compute the parameters. Helpful aids are also displayed during the issuance of a tsunami warning, such as, warning procedures; Rayleigh wave arrival times at various locations; and time elapsed from the origin time. Options are available for transferring data between monitors and for message generation. All seismic data are archived on disk for specified periods of time for later review and/or reprocessing.

All real-time processing PCs are networked together using the NT peer-to-peer LAN. In addition to the monitors described above, there are four more monitors dedicated to the WC/ATWC geographical information system (GIS) software developed at the WC/ATWC. Once an earthquake's parameters are determined, the GIS displays its location on both a global and smaller local map which are on separate monitors. The global map supports overlays of historical seismicity, tsunamis, plate boundaries, major cities, seismometers, tide gages, recent earthquakes, modeling results, and tsunami travel time contours. The localized map also supports many overlays, such as, cities, earthquakes ranked by magnitude and depth, roads, topography, pipelines, power lines, tide gages, seismometers, airports, railroads, place names, and tsunamis. Detailed information on historical earthquake and tsunami data bases (Lander *et al.*, 1989, Soloviev *et al.*, 1984) can be retrieved and viewed by clicking on an appropriate button.

Tsunami warnings, issued by the WC/ATWC, are of two types: regional warnings for tsunamis produced in or near the AOR and ones for tsunamis generated outside the AOR. Regional warnings are issued within 15 minutes of earthquake origin time and are based solely on seismic data. Warnings are issued for any coastal earthquake near the WC/ATWC's AOR over magnitude 7. Warnings outside the WC/ATWC's AOR are issued after coordination with the Pacific Tsunami Warning Center in Ewa Beach, Hawaii. These warnings are based on seismic data, along with historical tsunami records and recorded tsunami amplitudes from tide gages. Since 1981, 10 regional tsunami warnings have been issued by the WC/ATWC. The response times to issue a warning from the origin time of an earthquake ranges from 8-14 minutes with an average response of 10.6 minutes (Fig 1). Of these warnings, only two out of the ten occurred during the work day. All others occurred after normal work hours when the personnel were in standby duty status.

Tsunami warning messages are computer generated by interactively selecting from a menu of possible messages. Messages are composed automatically based on earthquake location, magnitude, and origin time. Appropriate earthquake parameters are automatically included in the messages, along with the tsunami ETAs for 24 coastal places in WC/ATWC's AOR The geophysicist can add to, or alter a message prior to dissemination. Messages are disseminated in several different ways. The primary methods are reading a message over the National Warning System (NAWAS); transmitting a message over the NOAA satellite system (NWWS); and transmitting it over a dedicated Federal Aviation Administration (FAA) teletype system. Messages read over the NAWAS phone are heard by emergency personnel from the federal to the county levels along the U.S. west coast and Alaska and by the U.S. Coast Guard stations. The NWWS transmits a printed copy of the message to the state emergency services, provincial emergency preparedness in British Columbia, Canada, and to other communication systems of the U.S. National Weather Service. The FAA teletype system is used to send a printed copy of the message to various governmental offices, military installations, and foreign countries. Secondary dissemination methods are e-mail, web page (www.alaska.net/~atwc), and phone calls.

In addition to tsunami warning messages, the WC/ATWC also issues information messages for earthquakes which may be felt strongly by local citizens but are not large enough to generate a tsunami. Each year, the WC/ATWC staff respond to more than 250 alarms averaging approximately five each week. These messages are important in preventing needless evacuations since citizens near coastal areas are taught to move to higher ground when severe earthquake shaking occurs. Other messages issued by the WC/ATWC include seismic data exchanges among other centers, and tsunami information messages for large earthquakes outside the AOR that are not potentially dangerous to the AOR.

Once a warning has been issued, the nearest tide gages are monitored to confirm the existence or nonexistence of a tsunami, and its degree of severity. The WC/ATWC has access to more than 90 tide sites throughout the Pacific Basin. Approximately 75% of these sites are maintained by NOAA's National Ocean Survey (NOS). In addition to the NOS sites, the remainder of the tide gage networks are operated by other agencies such as the Pacific Tsunami Warning Center, Japan Meteorological Agency, and others. The WC/ATWC maintains real-time telemetry equipment at seven NOS gages in Alaska and fully maintains an eighth tide gage at Shemya, Alaska. These eight gages provide real-time data sampled every 15 seconds, and transmitted via dedicated circuits to the WC/ATWC where

they are displayed on PC monitors.

The NOS sites' data are normally scheduled transmissions via satellite, every 1, 2 or 3 hours. The data are transmitted to the a satellite downlink on the U.S. east coast and then to the WC/ATWC over a dedicated circuit. In addition to the scheduled hourly transmissions of 6 minute data, there is dial-in capability to receive 1 minute data, transmitted every 5 minutes, for a period of 1 hour. Many of the NOS gages have tsunami triggering software at the site which enables immediate transmission of water level data if a tsunami has been detected. Software which was developed at the WC/ATWC displays the real-time water level data, triggered tsunami data, and the scheduled data transmissions on PC monitors. The scheduled transmission time is also shown on a graph displaying each sites' water level data. Superimposed upon the water level data is a marker-line indicating the expected tsunami arrival time for any given earthquake. The predicted tide and filtered tide is also shown for many sites. The tsunami warning is canceled or extended based on the information from the tide gages, historic tsunami records and pre-computed tsunami models

An on-going project at the WC/ATWC is the prediction of tsunami amplitudes outside the tsunami generating area (Whitmore and Sokolowski, 1996). The basic idea behind this technique is that pre-computed tsunami models can be scaled by recorded tsunami amplitudes during an earthquake to give a reasonable amplitude estimate outside the source zone. Tsunami models for moment magnitude 7.5, 8.2, and 9.0 earthquakes have been computed along the Pacific plate boundary from Honshu, Japan to the Cascadia subduction zone. The modeling technique was verified by comparison to historic tsunamis from the different regions. At present, the results from the scaled models are not distributed to the emergency officials during warnings, but are used internally as an aid in canceling or extending warnings.

Another current project at the WC/ATWC is to receive tsunami data from the Pacific-wide tide sites via a satellite phone system (Sokolowski *et al.*,1999). Due to the current delay of 1-3 hours in receiving tide data from NOS gages, selected windows of data can be received from these tide sites using a satellite phone, antennae, PC computer, and special hardware inserted into the current NOS field packages. This would permit a geophysicist at the WC/ATWC to review, via a PC, a window of data from selected tide sites nearest the tsunami source. A prototype is currently in development to test this concept. The software is nearing completion. The NOS tide site at Seward, Alaska, nearest the WC/ATWC, is being equipped with hardware which will enable the WC/ATWC to request and receive data which can be displayed by a PC. The advantages of this method over current methods are to: significantly decrease the current time delay of 1-3 hours; permit retrieval of tsunami data from gages for which there is no telephone dial-in; have reasonable costs; reduce/eliminate the need for costly dedicated circuits; not affect or impact the operations of another agency or center; and decrease the time that an area is placed in a warning while waiting for tide data to confirm the existence or non existence of a tsunami. Once this proof-of-concept is completed for one site, additional sites will follow as time and funding become available.

The ability of any warning system to successfully save lives and reduce property damage depends upon getting the information to the public and getting them to respond to the emergency. The WC/ATWC conducts a community preparedness program which provides advice and training sessions to coastal citizens and emergency managers to aid in pre-event planning. The aim of this

program is to educate the public to help themselves if they are caught in the middle of a violent earthquake and/or tsunami, and to be aware of safety procedures, safe areas, and the limitations of the Tsunami Warning System. All staff members participate in a three part preparedness effort which includes: visits to distant coastal communities from Adak to southern California; visits to local group facilities and schools that are within commuting distance of the WC/ATWC; and tours through the WC/ATWC's facilities. In addition to this on-going program, special visitations are made by the staff to the communities that were evacuated during an actual tsunami warning and no significant wave action materialized. The purpose of these visitations is to explain the warning actions to the public and to stress the continued need to respond to emergency tsunami warnings.

References

Johnson, C.E., Bittenbinder, A., Bogaert, B., Dietz, L., and Kohler, W, 1995, Earthworm: A flexible approach to seismic network processing, IRIS Newsletter, **14**, 1-4.

Lander, J.F. and P.A. Lockridge, 1989, United States Tsunamis, 1690-1989. U.S. Department of Commerce, NOAA, NESDIS, National Geophysical Data Center, Pub. 41-2, Boulder, CO.

Soloviev, S.L., and Go, Ch.N., 1984, Catalogue of tsunamis in the Pacific Ocean, Nauka Publishing House, Moscow.

Sokolowski, T. J., Fuller, G.W., Blackford, M.E. and Jorgensen, W.J., 1983, The Alaska Tsunami Warning Center's automatic earthquake processing system., Proceedings of the International Tsunami Symposium, IUGG, Hamburg, Germany.

Sokolowski, T. J., Medbery, A.H., and Urban, G.W., 1999 (Tsunami Data Retrieval by Satellite Telephone, in progress).

Veith, K.F. 1978, Seismic signal detection algorithm, Technical Note 1/78, Teledyne Geotech, 10 pp.

Whitmore, P.M. and Sokolowski, T.J.: 1996, Predicting tsunami amplitudes along the North American coast from tsunamis generated in the northwest Pacific during tsunami warnings, Science of Tsunami Hazards, **14**, 147-166.

Zitek, W.O., Medbery, A.H., and Sokolowski, T.J.: 1990, Concurrent seismic data acquisition and processing using a single IBM PS/2 computer, NOAA Technical Memorandum, NWS AR-40.

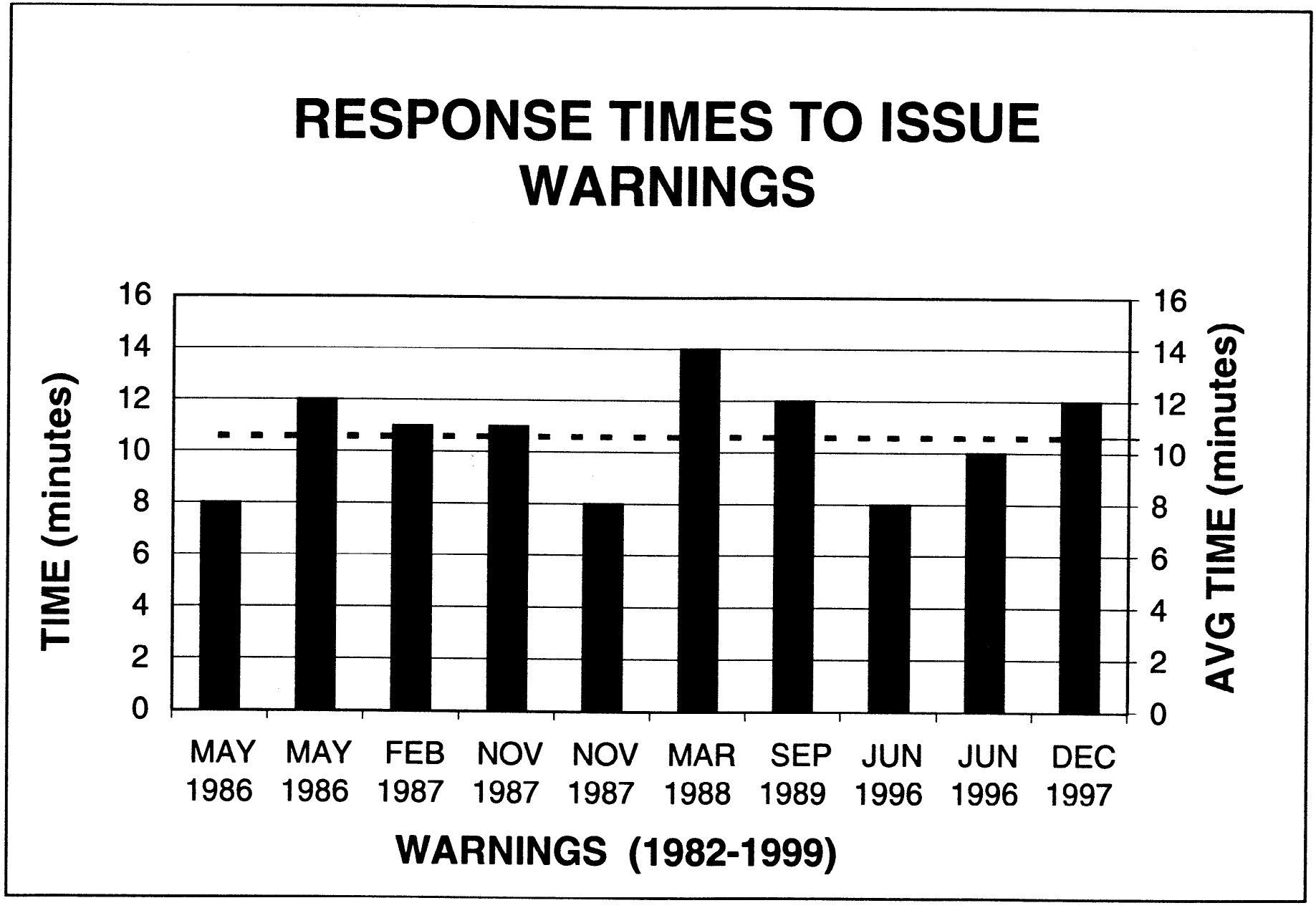

Figure 1. Shown are times in minutes to issue regional warnings by WC/ATWC since 1982.

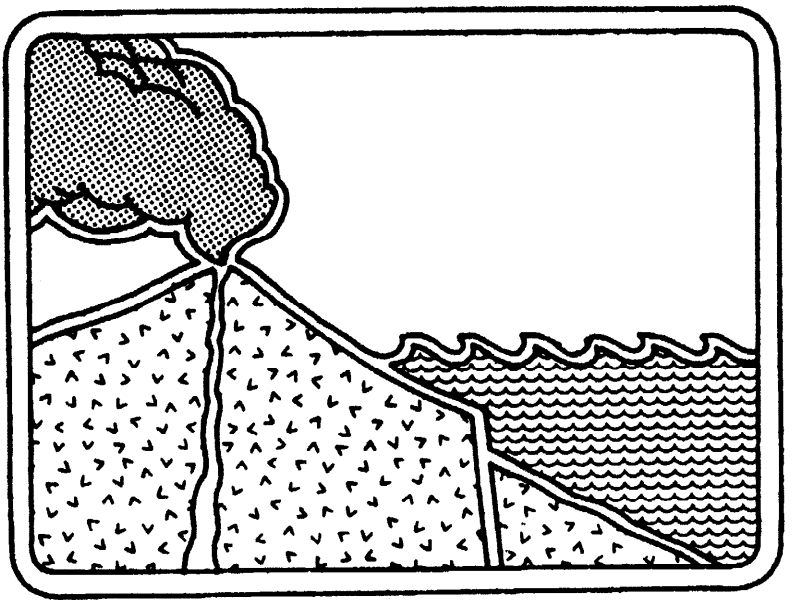

MODELING THE 1958 LITUYA BAY MEGA-TSUNAMI

Charles L. Mader
Los Alamos National Laboratory
Los Alamos, NM 87545 U.S.A.

ABSTRACT

Lituya Bay, Alaska is a T-Shaped bay, 7 miles long and up to 2 miles wide. The two arms at the head of the bay, Gilbert and Crillon Inlets, are part of a trench along the the Fairweather Fault. On July 8, 1958, an 7.5 Magnitude earthquake occurred along the Fairweather fault with an epicenter near Lituya Bay.

A mega-tsunami wave was generated that washed out trees to a maximum altitude of 520 meters at the entrance of Gilbert Inlet. Much of the rest of the shoreline of the Bay was denuded by the tsunami from 30 to 200 meters altitude.

The *SWAN* code which solves the nonlinear long wave equations was used to numerically model possible tsunami wave generation mechanisms.

A landslide of about 30 million cubic meters was probably triggered by the earthquake. It has been assumed to have been the source of the tsunami wave even though it was difficult to correlate with the eye-witness observations. Numerical studies indicated that the tsunami wave generated by a simple landslide gave tsunami wave inundations that were less than a tenth of those observed if the slide was assumed to lift a volume of water corresponding to the volume of the slide to above normal sea level.

Another possible source of the tsunami was a massive uplift of the sea floor along the Fairweather Fault that underlies the Gilbert and Crillon Inlets at the head of the bay. Even if all the water in the inlets was initially raised to above normal sea level, the observed tsunami inundations could not be numerically reproduced.

Dr. George Pararas-Caryannis suggested that tsunami wave was formed by a landslide impact similar to an asteroid impact making a cavity to the inlet ocean floor and a wave that splashed up to 520 meters height. If the run-up was 50 to 100 meters thick, adequate water is available between the slide and the run-up and the results are consistent with the observations. Further studies will require full Navier-Stokes modeling similar to those required for asteroid generated tsunami waves.

INTRODUCTION

Lituya Bay, Alaska is on the northeast shore of the Gulf of Alaska. It is an ice-scoured tidal inlet with a maximum depth of 220 meters and a narrow entrance with a depth of only 10 meters. It is a T-Shaped bay, 7 miles long and up to 2 miles wide. The two arms at the head of the bay, Gilbert and Crillon Inlets, are part of a trench along the the Fairweather Fault. On July 8, 1958, a 7.5 Magnitude earthquake occurred along the Fairweather fault with an epicenter near Lituya Bay.

A mega-tsunami wave was generated that washed out trees to a maximum altitude of 520 meters at the entrance of Gilbert Inlet. Much of the rest of the shoreline of the Bay was denuded by the tsunami from 30 to 200 meters altitude.

During the last 150 years 5 giant waves have occurred in Lituya. The previous event occurred on October 27, 1936 which washed out trees to a maximum altitude of 150 meters and was not associated with an earthquake.

Don Miller recorded all that was known in 1960 about the giant waves in Lituya bay in reference 1.

The July 9, 1958 earthquake occured at about 10:15 p.m. which is still daylight at Lituya Bay. The weather was clear and the tide was ebbing at about plus 5 feet. Bill and Vivian Swanson were on their boat anchored in Anchorage Cove near the western side of the entrance of Lituya Bay. Their astounding observations are recorded in reference 2 and were as follows:

"With the first jolt, I tumbled out of the bunk and looked toward the head of the bay where all the noise was coming from. The mountains were shaking something awful, with slide of rock and snow, but what I noticed mostly was the glacier, the north glacier, the one they call Lituya Glacier.

I know you can't ordinarily see that glacier from where I was anchored. People shake their heads when I tell them I saw it that night. I can't help it if they don't believe me. I know the glacier is hidden by the point when you're in Anchorage Cove, but I know what I saw that night, too.

The glacier had risen in the air and moved forward so it was in sight. It must have risen several hundred feet. I don't mean it was just hanging in the air. It seems to be solid, but it was jumping and shaking like crazy. Big chunks of ice were falling off the face of it and down into the water. That was six miles away and they still looked like big chunks. They came off the glacier like a big load of rocks spilling out of a dump truck. That went on for a little while – its hard to tell just how long – and then suddenly the glacier dropped back out of sight and there was a big wall of water going over the point. The wave started for us right after that and I was too busy to tell what else was happening up there."

A 15 meter high wave rushed out of the head of the bay toward Swanson's anchored boat. The boat shot upward on the crest of the wave and over the tops of standing spruce trees on the entrance spit of Lituya Bay. Swanson looked down on the trees growing on the spit and said he was more than 25 meters above their tops. The wave crest broke just outside the spit and the boat hit bottom and foundered some distance from the shore. Swanson saw water pouring over the spit, carrying logs and other debris. The Swansons escaped in their skiff to be picked up by another fishing boat 2 hours later.

The front of Lituya Glacier on July 10 was a nearly straight, vertical wall almost normal

to the trend of the valley. Comparisions with photographs of the glacier taken July 7 indicate that 400 meters of ice had been sheared off of the glacier front (reference 1).

The partially subglacial lake west of the sharp bend in Lituya glacier was 30 meters lower than it was 2 days before the earthquake (reference 1).

After the earthquake there was a fresh scar on the northeast wall of Gilbert Inlet, marking the recent position of a large mass of rock that had plunged down the steep slope into the water. The next day after the earthquake and tsunami, loose rock debris on the fresh scar was still moving at some places, and small masses of rock still were falling from the rock cliffs near the head of the scar. The dimensions of the slide on the slope are accurate but the thickness of the slide mass normal to the slope can only be estimated. The main mass of the slide was a prism of rock that was 730 meters and 900 meters along the slope with a maximum thickness of 90 meters and average thickness of 45 meters normal to the slope, and a center of gravity at about 600 meters altitude. As described in reference 1 this results in an approximate volume of 30 million cubic meters (40 million cubic yards).

Miller in reference 1 concluded that "the rockslide was the major, if not the sole cause of the 1958 giant wave." The 1958 tsunami has been accepted in the technical literature as landslide generated. The Swanson observations have not been believed as they indicate that a lot more than a simple landslide occurred.

MODELING

The generation and propagation of the tsunami wave of July 8, 1958 in Lituya Bay was modeled using a 92.75 by 92.75 meter grid of the topography. The modeling was performed using the *SWAN* non-linear shallow water code which includes Coriolis and frictional effects. The *SWAN* code is described in reference 3. The calculations were performed on a 200 Mhz Pentium personal computer. The 3 by 6 second land topography was generated from the Rocky Mountain Communication's CD-ROM compilation of the Defense Mapping Agency (DMA) 1 x 1 degree blocks of 3 arc second elevation data. The sea floor topography was taken from sea floor topographic maps published in reference 1. The grid was 150 by 150 cells and the time step was 0.15 second.

SIMPLE LANDSLIDE MODEL

The landslide described by Miller in reference 1 had an approximate volume of 30 million cubic meters and was 730 meters wide. To model the maximum expectable tsunami that could be generated by the landslide, it was assumed that the landslide uplifted the water in front of the slide by the depth of the water until 30 million cubic meters of water was uplifted. The uplift was assumed to occur instantaneously and at various velocities. The slide extended about 800 meters into Gilbert inlet and the maximum uplift of water was 120 meters which is the maximum depth of the inlet. The initial landslide geometry and the maximum inundation limit are shown in Figure 1. The inundation limits are less than a tenth of those that occurred.

EARTHQUAKE MODEL

The simple landslide model suggested that a much larger volume of water needed to be displaced to generate the mega-tsunami than could be displaced by the landslide. The earthquake model assumes that all the water in the head of the bay including Gilbert and Crillon Inlets is uplifted by the depth of the water. Figure 2 shows the initial region assumed to be uplifted by the earthquake along the Fairweather Fault. The maximum height of the uplifted water was 120 meters. Also shown in Figure 2 is the inundation limit which is much less than observed.

LAKE MODEL

Since a much larger source of water than was available in the inlet appeared to be required, one possible source was the large partially subglacial lake west of the sharp bend in Lituya glacier which flows down Gilbert inlet. The level of the lake was observed to have lowered 30 meters after the earthquake. The lake is at about 300 meter altitude.

To reproduce the flooding outside the head of the bay, a wall of water 200 meters high had to flood all of Gibert inlet. The wall of water was given an initial velocity of 35 meters/second. It was also assumed that the uplift from the simple landslide occurred simultaneously although it had no significant effect. Figure 3 shows the initial region flooded to 200 meters by the water from the lake and the inundation limit which is similar to that observed outside the head of the bay.

The lake model does not generate the mega-tsunami that washed out trees to a maximum altitude of 520 meters at the entrance of Gilbert Inlet. It seems unlikely that the lake could have drained fast enough to have produced the required wall of water.

LANDSLIDE IMPACT MODEL

The Swanson observations suggest a water wave lifted the front of the glacier up and moved it out from its initial position and generated the 520 meter high wave run-up.

George Pararas-Caryannis suggested that the wave was formed by a landslide impact similar to an asteroid impact, making a cavity in the inlet ocean to the depth of the inlet floor (120 meters) near the landslide.

The water in the inlet with the width of the landslide and between the landslide and the 520 meter high run-up is sufficient to cover the the run-up region to 100 meter height. This high water layer is sufficient to form a wave that will reproduce the observed flooding of the bay beyond the inlet. The calculated source and inundation limit is shown in Figure 4.

The P.C. landslide impact model will require full Navier-Stokes modeling similar to that required for asteroid generated waves.

CONCLUSIONS

The mega-tsunami that occurred on July 9, 1958 in Lituya Bay washed out trees to a maximum altitude of 520 meters at the entrance of Gilbert Inlet. Much of the rest of the shoreline of the Bay was denuded by the tsunami from 30 to 200 meters altitude.

The amount of water displaced by a simple landslide or an earthquake along the Fairweather fault at the head of the bay is insufficient to cause the observed tsunami wave. The water in the glacial lake is a possible source of the large volume of water required.

To reproduce the flooding outside the head of the bay, a wall of water 200 meters high had to flood all of Gibert inlet. The lake model does not generate the mega-tsunami that washed out trees to a maximum altitude of 520 meters at the entrance of Gilbert Inlet. To generate such a tsunami that also reproduces the Swanson observations of the movement of the Lituya Bay glacier face, Dr. George Pararas-Caryannis suggested a landslide impact similar to an asteroid impact. Such a model can be made consistent with the observations. The P.C. landslide impact model will require full Navier-Stokes modeling similar to that required for asteroid generated waves.

Since the Miller report (reference 1) which documents the Lituya Bay tsunamis is difficult to obtain, Figure 5 and 6 reproduce the figures showing the upper limit of destruction of forest and a photograph of where the wave reached 520 meters.

The Tlingit natives believe that a powerful spirit, Kah Lituya, lives in deep ocean caverns near the entrance to the bay. He resents being disturbed and rises up to shake the mountains and wash away intruders with giant waves.

Los Alamos National Laboratory Contribution LA-UR-99-1572

REFERENCES

1. Don J. Miller, "Giant Waves in Lituya Bay, Alaska" Geological Survey Professional Paper 354-C, U. S. Government Printing Office, Washington (1960).
2. Frances E. Calwell, **Land of The Ocean Mists-The Wild Ocean Coast West of Glacier Bay**, Alaska Northwest Publishing Company, Edmonds, Washington ISBN 0-88240-311-7 (1986).
3. Charles L. Mader, **Numerical Modeling of Water Waves,** University of California Press, Berkeley, California (1988).

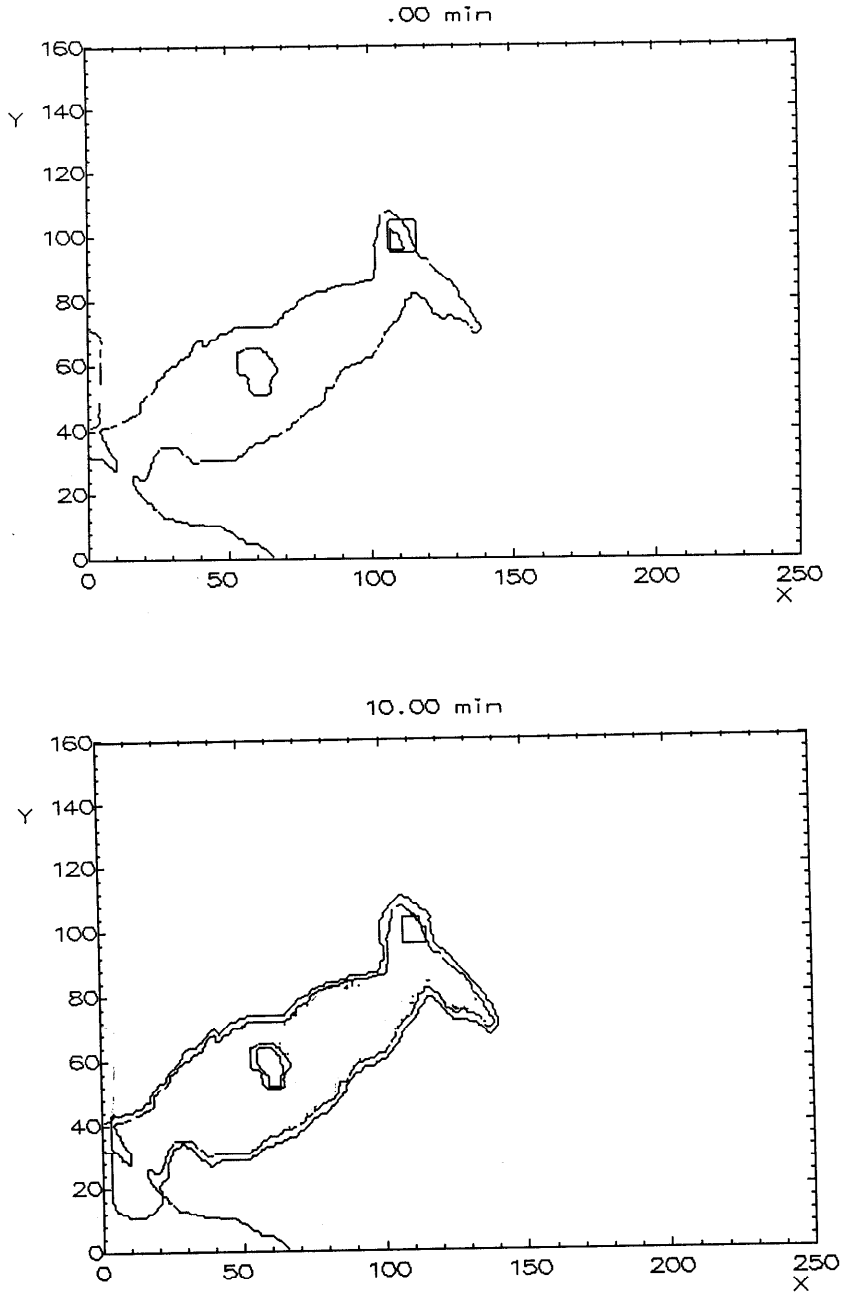

Figure 1. The landslide source and inundation limit.

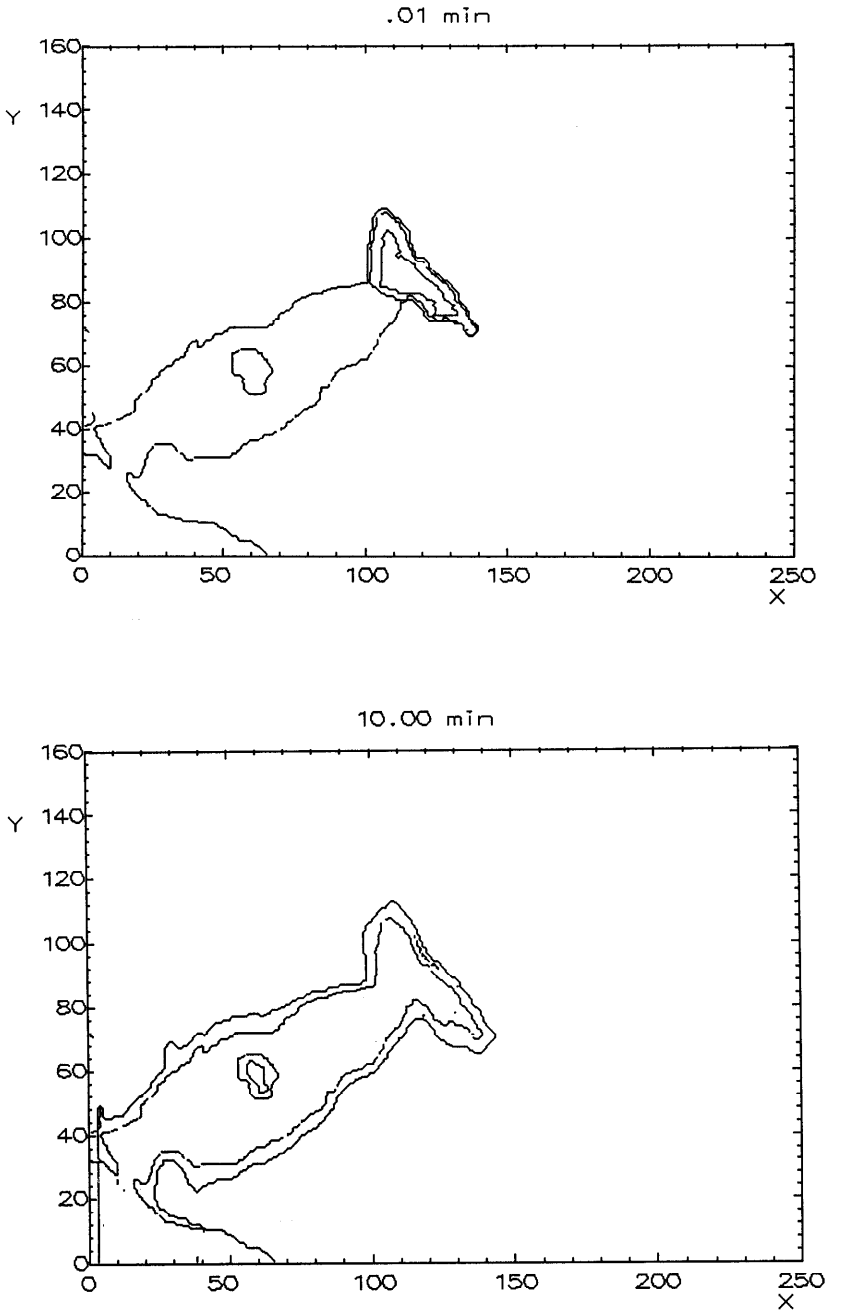

Figure 2. The earthquake source and inundation limit.

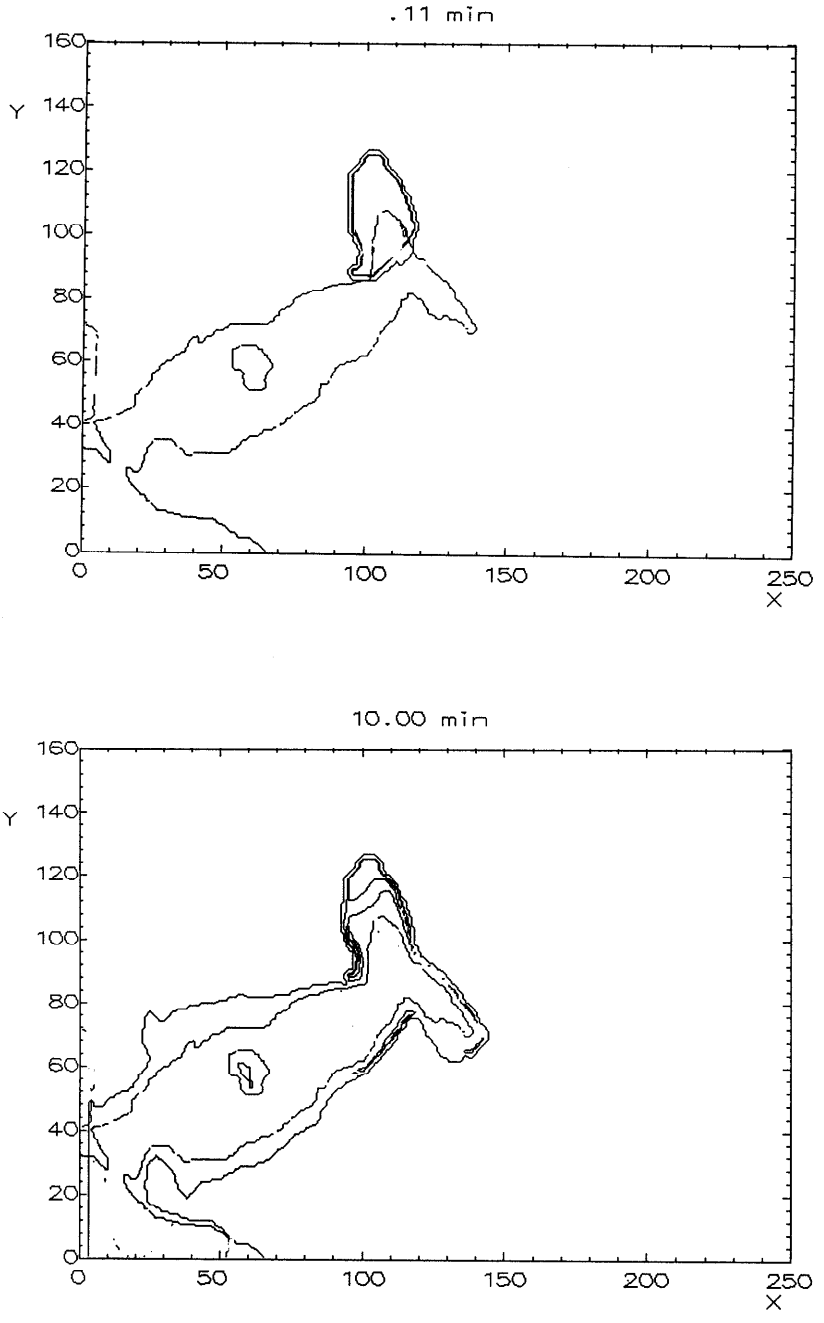

Figure 3. The Lake Drainage Source and inundation limit.

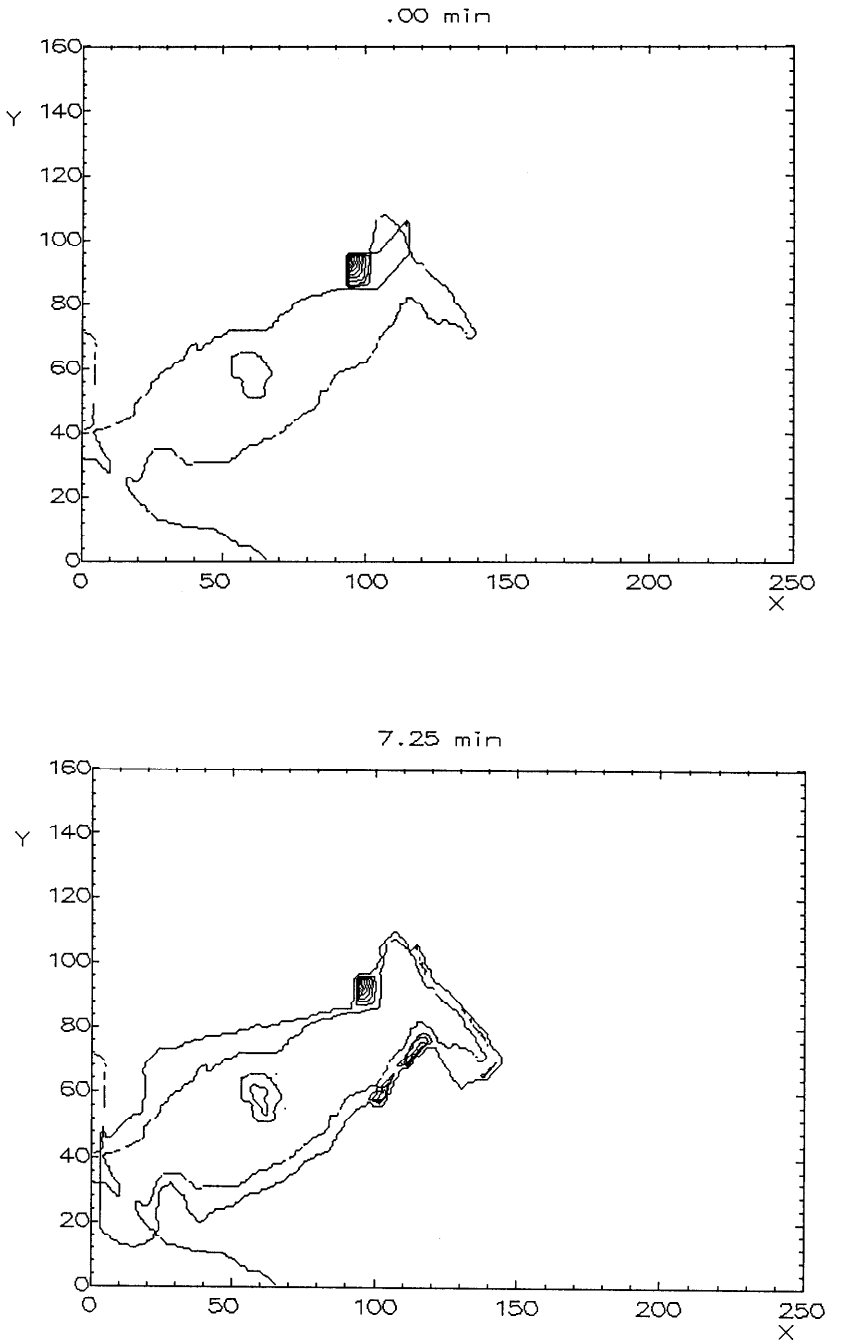

Figure 4. The P. C. Impact Landslide source and inundation limit.

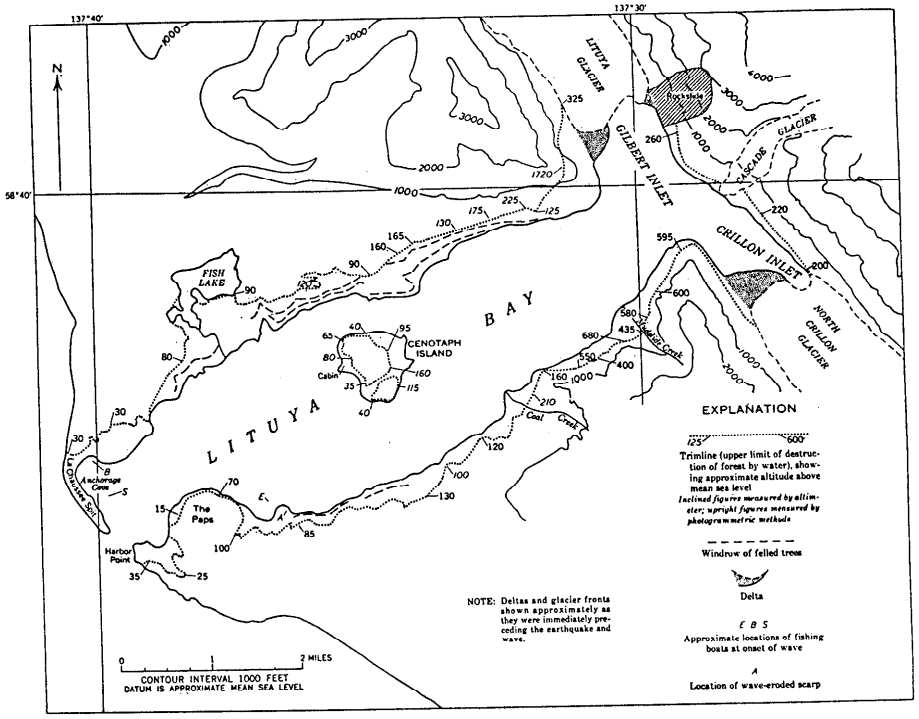

Map of Lituya Bay showing setting and effects of 1958 giant wave.

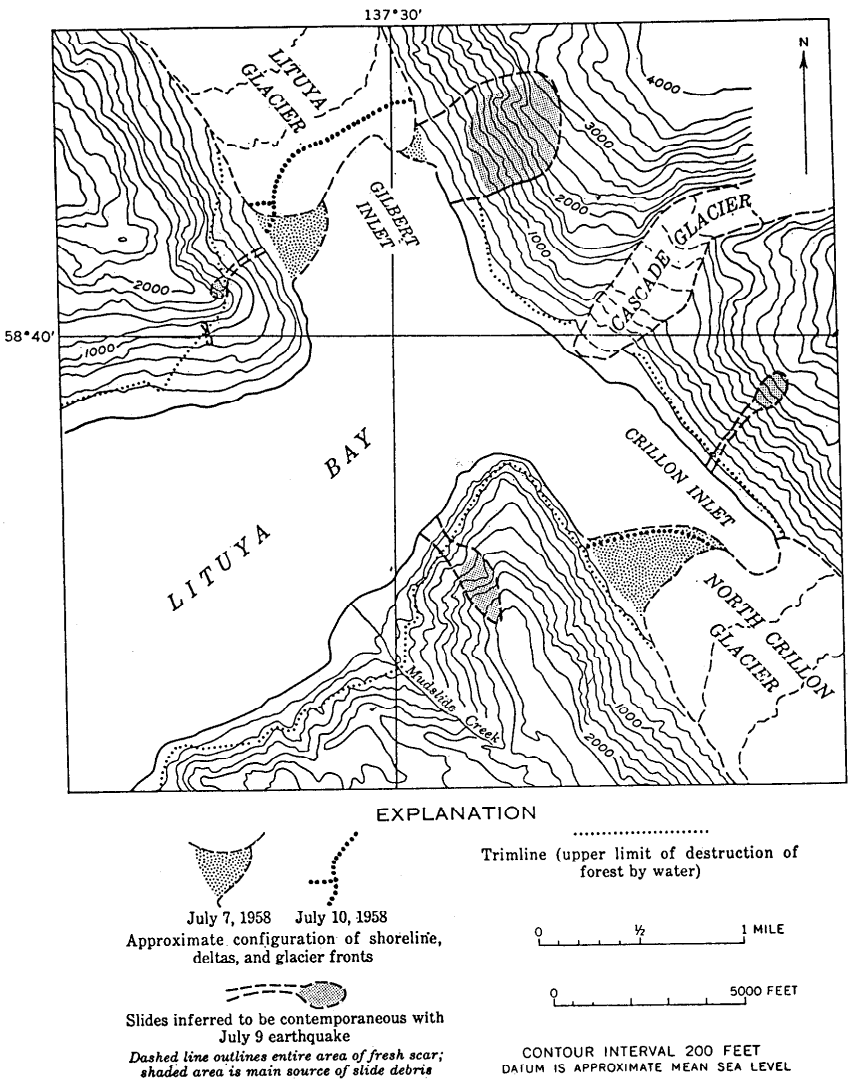

--Detailed map of head of Lituya Bay, showing slides, changes in the shoreline and glacier fronts, and trimlines resulting from the 1958 earthquake and giant wave.

Figure 5.

Taken on August 29, 1958, this view of the spur ridge going into Gilbert Inlet shows where the giant wave reached 1,720 feet high. The camera is looking northwest at the head of Lituya Bay.
Photo by D.J. Miller.

Figure 6.

APPLICATION FOR MEMBERSHIP

THE TSUNAMI SOCIETY
P. O. Box 25218
Honolulu, Hawaii 96825, USA

I desire admission into the Tsunami Society as: (Check appropriate box.)

☐ Student ☐ Member ☐ Institutional Member

Name _____ Signature _____

Address _____ Phone No. _____

_____

Zip Code _____ Country _____

Employed by _____

Address _____

Title of your position _____

FEE: Member $25.00 Institution $100.00

Fee includes a subscription to the society journal: SCIENCE OF TSUNAMI HAZARDS.

Send dues for one year with application. Membership shall date from 1 January of the year in which the applicant joins. Membership of an applicant applying on or after October 1 will begin with 1 January of the succeeding calendar year and his first dues payment will be applied to that year.